IEEE Access
Multidisciplinary | Rapid Review | Open Access Journal

Received 12 April 2023, accepted 15 May 2023, date of publication 18 May 2023, date of current version 6 June 2023.

Digital Object Identifier 10.1109/ACCESS.2023.3277537

RESEARCH ARTICLE

Design of Missile Guidance Law Using Takagi-Sugeno-Kang (TSK) Elliptic Type-2 Fuzzy Brain Imitated Neural Networks

DUC-HUNG PHAM[1,2], CHIH-MIN LIN[1], VAN NAM GIAP[3], VAN-PHONG VU[4], AND HSING-YUEH CHO[1]

[1]Department of Electrical Engineering, Yuan Ze University, Taoyuan 320, Taiwan
[2]Faculty of Electrical and Electronic Engineering, Hung Yen University of Technology and Education, Hai Duong 160000, Vietnam
[3]School of Electrical and Electronic Engineering, Hanoi University of Science and Technology, Hai Ba Trung, Hanoi 100000, Vietnam
[4]Department of Automatic Control, Ho Chi Minh City University of Technology and Education, Ho Chi Minh City 70000, Vietnam

Corresponding authors: Duc-Hung Pham (phamduchung@saturn.yzu.edu.tw) and Chih-Min Lin (cml@saturn.yzu.edu.tw)

This work was supported by the Ministry of Science and Technology of Taiwan under Grant MOST 109-2221-E-155-027-MY3.

ABSTRACT The exploiting of missile guidance law is one of the most important issue of defense systems. However, it is a complex nonlinear guidance control problem. In recent years, several intelligent algorithms have been employed for the missile guidance law design. This paper aims to provide a more effective intelligent neural network, and then apply it to missile guidance control. An elliptic type-2 function (ET2F) combined with a Takagi-Sugeno-Kang (TSK) fuzzy system (FS) based on a wavelet function and a brain imitated neural network (BINN) is proposed to produce a new Takagi-Sugeno-Kang elliptic type-2 fuzzy brain imitated neural network (TSKET2FBINN). The proposed TSKET2FBINN is then incorporated into the missile guidance law. The proposed missile guidance control system includes the TSKET2FBINN controller and a robust compensation controller. A Lyapunov function is used to generate parameter adjustment adaptive laws so as to guarantee system stability with fast tracking performance of missile guidance control system. By presenting three missile control scenarios, the effectiveness of the proposed method is then demonstrated. The miss-distance (MD) of the proposed method is calculated and compared to other recent guidance methods to demonstrate its superior performance.

INDEX TERMS Elliptic type-2 function, TSK fuzzy system, brain imitated neural network, missile guidance law, command to line-of-sight.

I. INTRODUCTION

The exploiting of missile guidance law is one of the most important issue of defense systems. The idea behind the command to line-of-sight (CLOS) is to keep the missile pursuing and target in visual contact until impacting time [1]. There are numerous advantages for following the CLOS guidance law. First, using this rule can eliminate the need for a costly searching mechanism. Second, unlike the well-known proportional navigation, it does not rely on information about the range of the target, which makes it completely insensitive to interference. Third, in some scenarios where the target and tracker must be kept within a single narrow beam due to radar constraints, so a CLOS guidance law is required. In addition, as the precision of ground tracker increases, the CLOS-law becomes more desirable, especially for short-range air defense systems. Nevertheless, there are few scientific works that address the specifics of this guidance law. Lin and Peng demonstrated how to solve the nonlinear tracking problem of CLOS guidance control using a cerebellar model articulation controller [1]. Lin and Wang proposed a fuzzy side force control for missile against hypersonic target [2]. Wang and Hung [3] presented a fuzzy neural network (FNN) missile guidance control system in 2013,

The associate editor coordinating the review of this manuscript and approving it for publication was Min Wang.

in which the proposed FNN controller's weighting factors are used to direct the defending missile (DM) toward the attacking missile (AM). Wang et al. [4] proposed an adaptive self-organizing map (SOM) controller with recurrent neural network (RNN) in 2014 for missile defense systems (MDS). Li et al. [5] published a model predictive control using a constrained quadratic programming (QP) problem and a neural network for guidance control law in 2015.

Recently, neural networks (NNs) have been successfully applied in nonlinear system [6], especially for aerospace engineering [7], NN for steering law for manoeuvring targets [8], NN of missile guidance control [9]. Su et al. presented a guidance law in [8], which was developed using the backstepping method of sliding mode control, a radial basis function (RBF) neural network, and an adaptive control technique. A Lyapunov-based stability analysis shows that all signals are bounded and the LOS rates eventually converge near the origin. Liang et al. proposed NN-based nonlinear integrated missile control in conjunction with a disturbance observer [9]. Fuzzy neural also applied in latest application such as control of waverider vehicles [10], [11]. Bu et al. [10] proposed a new nonfragile prescribed performance control method for waverider vehicles (WVs) such that the quantitative prescribed performance can be guaranteed for tracking errors in the presence of actuator saturation. In this design, low-complexity fuzzy neural control protocols are presented for velocity subsystem and altitude subsystem of WVs. Also, Bu et al. [11] presented A fuzzy-neural-approximation-based pseudo non-affine control protocol for waverider vehicles (WVs), which is capable of guaranteeing tracking errors with desired prescribed performance and rejecting the obstacle of fragility inherent in the traditional prescribed performance control.

The first type of fuzzy logic systems is called a type-1 system, and the second type is called a type-2 system. Since type-1 fuzzy logic systems usually have accurate membership functions, type-1 fuzzy neural networks (FNNs) and fuzzy BELCs cannot account for the uncertainty of the rules. However, many external and internal disturbances are unavoidable and occur in many practical applications. Type-2 fuzzy logic systems, an extension of type-1 fuzzy logic systems used for FNNs and fuzzy BELCs [12], [13], have been proposed to mitigate the effects of such uncertainties. Type-2 fuzzy elliptic functions are more general, and can control the fuzzy footprint, manage and represent uncertainties, and make decisions with incomplete or ambiguous data [14]. In type-2 fuzzy elliptic functions, the form of the fuzzy ''footprint'' is the membership function. Type reduction methods, such as the Karnik-Mendel scheme [15], can convert type-2 fuzzy BELCs into type-1 fuzzy BELCs, but they are very computationally intensive. In addition, type-2 fuzzy elliptic functions do not explain the concept of variability and cannot model the diversity of opinions of a single expert or a group of experts. The nonstationary fuzzy set theory and the corresponding nonstationary fuzzy inference system were introduced [16]. This step was taken in response to the shortcomings of type-2 fuzzy inference systems. Moreover, an iterative algorithm for interval fuzzy sets of type-2 was proposed, which reduces the nature of the stopping condition. This algorithm, based on the Karnik-Mendel scheme, starts with the initialization of the switching point and then proceeds to a unidirectional search [17]. The parameters responsible for the support and the width are intertwined, which is a general drawback of membership functions of type-2 fuzzy systems. When using an elliptic membership function of type-2, the parameters responsible for the width of the fuzziness can be separated from those responsible for the support and the center of the membership function. In addition, elliptic membership functions have specific values for the left and right ends of the support, but ignore the blur on the rest of the support [14], [17]. This is due to the fact that elliptic membership functions are elliptic. These properties can be used to study how the presence of fuzziness in the input affects the inference of type-2 fuzzy logic systems.

There are two types of fuzzy systems: Takagi-Sugeno-Kang (TSK) fuzzy systems (FS) and Mamdani-Larsen fuzzy systems [18], [19]. The TSK fuzzy inference model can improve mapping and achieve accurate approximation performance, making it more useful for a wide range of applications. Zhao and Lin [19] proposed a wavelet-TSK-type fuzzy cerebellar model neural network (WTFCMNN), which combines a Gaussian-type FCMNN and a TSK- fuzzy inference system based on a wavelet function. In the subsequent portion of each rule, the TSK fuzzy inference system employs the series expansion of wavelet functions rather than the linear combination of input functions. Using this property, wavelet functions can easily obtain the global and local behaviour of any function [20]. Consequently, this paper employs the TSK fuzzy system based on a wavelet function.

Nevertheless, wavelet-function-based fuzzy systems have been reported in a number of prior studies, including flight control [11], [21], [22], [23]. In comparison with them, this paper used wavelet function based TSK fuzzy system to replace the traditional first-order linear function. The wavelet function acts as a connected function between the inputs and the weight spaces. Therefore, this makes special improvement in comparison with the wavelet-function-based fuzzy systems in [11], [21], [22], and [23].

The imprecision of system uncertainties and external perturbations is a constant challenge for researchers working with nonlinear control systems. The brain imitated neural network (BINN) was developed by Lucas et al. [24] to address these issues. The components of the BINN are: Input, Learning, Output, Emotion, Emotion Output, and Controller Output. By combining with other systems such as CMAC [13], [25], function-link [26], TSK fuzzy system [13], [27], wavelet type-2 fuzzy system [13], and type-2 fuzzy system [28], the performance of BINN can be improved.

Therefore, in this paper, a new neural network (NN) using the type-2 elliptic function, TSKFS, and BINN is

TABLE 1. A comparison of the proposed structure and the related works.

	Method	Contribution	Compensation controller	Additional methods	Membership function	Parameter learning of weights	Stability convergence method
1	The proposed TSKET2FBINN	Takagi–Sugeno–Kang elliptic type-2 fuzzy brain imitated neural network	Robust compensator	Exploiting sliding mode control (SMC)	Exploiting an elliptic type-2 membership function	Exploiting TSK fuzzy adaptive weights based on wavelet function, which can be updated online by adaptive laws.	Exploiting the gradient descent method
2	DFLFBC [26]	Double function-link fuzzy brain imitated neural network	None	Exploiting SMC	Exploiting the wavelet function	Exploiting adaptive weights	Exploiting the gradient descent method
3	WIT2FBCC [13]	Wavelet interval type-2 fuzzy hybrid controller	Exploiting robust controller	Exploiting SMC	Exploiting interval wavelet type-2 function	Exploiting adaptive weights	Using a Lyapunov function
4	T2HC [28]	Type-2 fuzzy fuzzy cerebellar model articulation controller brain imitated neural network	Exploiting H-infinity robust compensator	Exploiting sliding mode controller.	Exploiting the Gaussian function	Exploiting adaptive dynamic weights	Exploiting a Lyapunov function.
5	PD-ET2FNN [17]	Type-2 fuzzy neural networks with elliptic membership functions	Exploiting a robust compensator	Exploiting sliding mode controller.	Exploiting a type-2 fuzzy elliptic membership function	Exploiting adaptive weights	Exploiting a Lyapunov function
6	AC-IT2-TSK-FNN [29]	Actor-critic - interval type-2 TSK fuzzy neural network	none	Exploiting a novel structure for actor-critic	Exploiting interval type 2 elliptic membership function	Exploiting adaptive weights based on the TSK fuzzy system	The parameters updated based on a cost function and fuzzy clustering
7	RWBEL [30]	Recurrent wavelet based brain imitated neural network	Exploiting a robust compensator	Exploiting sliding mode controller.	Exploiting Wavelet function	Exploiting adaptive weights	Exploiting a Lyapunov function

presented. It is called the Takagi-Kang-Sugeno elliptic type-2 fuzzy brain imitated neural network (TSKET2FBINN). The proposed structure includes the advantages of a type-2 elliptic membership function, a BINN, and a TSK fuzzy inference system. Then, the proposed structure is a more general type-2 fuzzy neural network. If the number layer of the TSKET2FBINN is reduced to one and each block has only one neuron, and the type-2 elliptic membership function is replaced by another membership function, then the structure can be called a TSK type-2 fuzzy neural network.

The exploiting of missile guidance law is one of the most important issue of defense systems. However, it is a complex nonlinear guidance control problem. In recent years, several intelligent algorithms have been employed for the missile guidance law design. This paper aims to provide a more effective intelligent neural network, and then apply it to missile guidance control.

To control the missile, a suitable control law can be designed. Since the target is in motion, the line-of-sight (LOS) may shift at any time, and the target is flying with an unknown acceleration. The anti-aircraft missile is generally controlled by a system that tracks the targets. However, the control target is the distance between the missile and the intended target. This is because the detected target is in motion and may be subject to unexpected escaping acceleration [1]. The TSKET2FBINN is developed for the purpose of evaluating the effectiveness of this guidance system. Thus, this paper aims on applying the proposed TSKET2FBINN control system for missile guidance control law design to significantly improve the system performance. Finally, three scenarios of missile guidance control are used to show the performance and effectiveness of the proposed TSKET2FBINN. Moreover, a comparison of the proposed structure and the related works is presented in Table 1.

The main contributions of this work are listed below:

(1) An elliptic type-2 function (ET2F) [14], [15], [16], [17] along with a Takagi-Sugeno- Kang fuzzy system [18], [19] and a brain imitated neural network

(BINN) [24] are incorporated to improve response to input uncertainties.
(2) The updated weight of the TSK application is based on the wavelet function, which increases the flexibility of the automatic parameter updating [18], [19], [20].
(3) A missile guidance control law based on the proposed TSKET2FBINN is designed and its performance is evaluated through three simulation scenarios in section V of the paper.
(4) Utilizing miss-distance (MD) calculation and t-test statistical evaluation to compare the proposed method with other previous methods in the end of section V of the paper can illustrate the effectiveness of the proposed guidance law.

The rest of this article is structured as follows. Problem formulation is given in section II, the proposed TSKET2FBINN is described in section III, convergence analysis and online learning rules is presented in section IV, Simulation results for the proposed missile guidance strategy are presented in section V, and finally the conclusion of the paper is given in section VI.

II. PROBLEM FORMULATION

It is possible to solve the 3-dimensional CLOS control problem by applying techniques from the tracking problem for a time-varying nonlinear system. A three-dimensional diagram for tracking a missile on its way to its target is described in Figure 1 [1]. The ground tracker is the starting point for the inertial measurement unit. Both the axis and the plane are at 90 degrees to each other. The body frame of the rocket rotates about the center of mass with the axis pointing forward along the centerline of the rocket. The inertial frame of the rocket is represented by the following equations [1], [2], [3], [4], (1) as shown at the bottom of the page, where $\begin{pmatrix} x_m & y_m & z_m \end{pmatrix}$ is missile position in inertial frame, ψ_m is yaw angle of missle, θ_m is pitch angle of missle, ϕ_{mc} is roll angle command, g is gravity acceleratio, a_x is axial acceleration of missile, a_{yc} is yaw acceleration of command, a_{zc} is pitch acceleration of command, R_m is missile range from ground tracker, v_m is missile velocity, $s\theta$ is sin (θ), and $c\theta$ is cos (θ).

The 3-D CLOS guidance problem is posed as a tracking problem. The guidance requirement is to control the missile always pressing on the LOS and keeping forward in order to hit the target. However, due to instrument errors, target movement, and thrust direction errors, the missile guidance

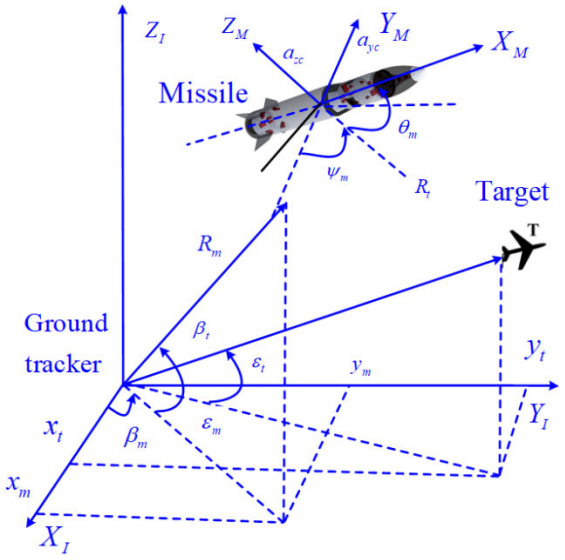

FIGURE 1. 3-D missile target tracking scheme.

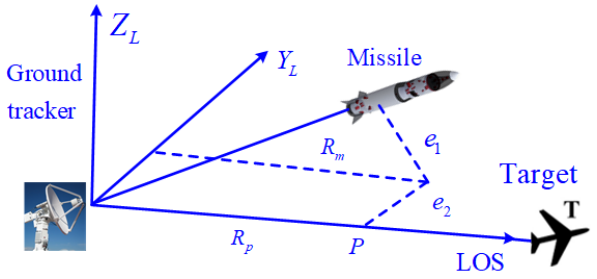

FIGURE 2. Definition of tracking error in LOS frame.

system cannot always stay on the LOS between the missile and the target. The tracking error LOS frame is shown in Fig. 2. The axis is horizontally to the left of the aircraft and points forward along the line of sight to the target. The rotational relationships between the coordinates of the missile's LOS frame is described in figure 2, which are as follows [1]:

$$\begin{bmatrix} e_1 \\ e_2 \end{bmatrix} = \begin{bmatrix} -\sin(\beta_t) & \cos(\beta_t) & 0 \\ -\sin(\varepsilon_t)\cos(\beta_t) & -\sin(\varepsilon_t)\sin(\beta_t) & \cos(\varepsilon_t) \end{bmatrix} \begin{bmatrix} x_m \\ y_m \\ z_m \end{bmatrix} \tag{2}$$

where β_t, ε_t are respectively azimuth angle of LOS to target and elevation angle of LOS to target.

$$\begin{bmatrix} \ddot{x}_m \\ \ddot{y}_m \\ \ddot{z}_m \end{bmatrix} = \begin{bmatrix} c\theta_m c\psi_m & -s\phi_{mc}s\theta_m c\psi_m - c\phi_{mc}s\psi_m & -c\phi_{mc}s\theta_m c\psi_m + s\phi_{mc}s\psi_m \\ c\theta_m s\psi_m & -s\phi_{mc}s\theta_m c\psi_m + c\phi_{mc}s\psi_m & -c\phi_{mc}s\theta_m s\psi_m - s\phi_{mc}s\psi_m \\ s\theta_m & s\phi_{mc}c\theta_m & c\phi_{mc}c\theta_m \end{bmatrix} \cdot \begin{bmatrix} a_x \\ a_{yc} \\ a_{zc} \end{bmatrix} - \begin{bmatrix} 0 \\ 0 \\ g \end{bmatrix}$$

$$\begin{bmatrix} \dot{\psi}_m \\ \dot{\theta}_m \end{bmatrix} = \begin{bmatrix} \frac{c\phi_{mc}}{(v_m c\theta_m)} & \frac{s\phi_{mc}}{(v_m c\theta_m)} \\ \frac{s\phi_{mc}}{v_m} & \frac{c\phi_{mc}}{v_m} \end{bmatrix} \cdot \begin{bmatrix} a_{yc} \\ a_{zc} \end{bmatrix} - \begin{bmatrix} 0 \\ \frac{gc\theta_m}{v_m} \end{bmatrix} \tag{1}$$

Specifically, we have a tracking error $\boldsymbol{e} \equiv [e_1, e_2]^T$. Since e_1 and e_2 are impossible to measure and directly, these quantities must be calculated by transforming the rocket's polar position data, which can be retrieved from the ground tracker, into a known coordinate system.

$$\begin{aligned}\boldsymbol{e} &\equiv \begin{bmatrix} e_1 \\ e_2 \end{bmatrix} \\ &= \begin{bmatrix} R_m \cos(\Delta\varepsilon + \varepsilon_t)\sin(\Delta\beta) \\ R_m \sin(\Delta\varepsilon+\varepsilon_t)\cos(\gamma_t) - R_m \cos(\Delta\varepsilon+\varepsilon_t)\sin(\varepsilon_t)\cos(\Delta\beta) \end{bmatrix}\end{aligned} \tag{3}$$

where $\boldsymbol{e}$ is the distance between the launch point of the missile and the line of sight. Thus, if the tracking errors can be controlled to be reduced to zero before the target crosses the missile, the missile will eventually hit the target. The 3-dimensional (3-D) CLOS steering challenge has been reformulated into a tracking problem. Define

$$\begin{aligned} x &\equiv \begin{bmatrix} x_1 & x_2 & x_3 & x_4 & x_5 & x_6 & x_7 & x_8 \end{bmatrix}^T \\ &\equiv \begin{bmatrix} x_m & y_m & z_m & \dot{x}_m & \dot{y}_m & \dot{z}_m & \psi_m & \theta_m \end{bmatrix}^T \\ u_T &\equiv \begin{bmatrix} u_{T1} & u_{T2} \end{bmatrix}^T \equiv \begin{bmatrix} a_{yc} & a_{zc} \end{bmatrix}^T \end{aligned} \tag{4}$$

Using the above notation, equations (1) and (3) can be converted into the following state space form:

$$\begin{aligned} \dot{\boldsymbol{x}} &= \boldsymbol{f}(x) + \sum_{o=1}^{2} \boldsymbol{g}_o u_{To} \\ \boldsymbol{e} &= \boldsymbol{h}(x) \end{aligned} \tag{5}$$

where

$$\boldsymbol{f}(x) = \begin{bmatrix} x_4 \\ x_5 \\ x_6 \\ a_x \cos(x_7)\cos(x_8) \\ a_x \sin(x_7)\cos(x_8) \\ a_x \sin(x_8) - g \\ 0 \\ -\dfrac{g\cos(x_8)}{\left(x_4^2 + x_5^2 + x_6^2\right)^{1/2}} \end{bmatrix} \in \Re^{8\times 1} \tag{6}$$

$$g_1(x) = \begin{bmatrix} 0 \\ 0 \\ 0 \\ -\sin(\phi_{mc})\sin(x_8)\cos(x_7) - \cos(\phi_{mc})\sin(x_7) \\ -\sin(\phi_{mc})\sin(x_8)\sin(x_7) + \cos(\phi_{mc})\sin(x_7) \\ \sin(\phi_{mc})\cos(x_8) \\ \dfrac{\cos(\phi_{mc})}{\left(x_4^2 + x_5^2 + x_6^2\right)^{1/2}\cos(x_8)} \\ \dfrac{\sin(\phi_{mc})}{\left(x_4^2 + x_5^2 + x_6^2\right)^{1/2}} \end{bmatrix} \in \Re^{8\times 1}$$

$$g_2(x) = \begin{bmatrix} 0 \\ 0 \\ 0 \\ -\cos(\phi_{mc})\sin(x_8)\cos(x_7) + \sin(\phi_{mc})\sin(x_7) \\ -\cos(\phi_{mc})\sin(x_8)\sin(x_7) - \sin(\phi_{mc})\sin(x_7) \\ \cos(\phi_{mc})\cos(x_8) \\ -\dfrac{\sin(\phi_{mc})}{\left(x_4^2 + x_5^2 + x_6^2\right)^{1/2}\cos(x_8)} \\ \dfrac{\cos(\phi_{mc})}{\left(x_4^2 + x_5^2 + x_6^2\right)^{1/2}} \end{bmatrix} \in \Re^{8\times 1} \tag{7}$$

$$\begin{aligned} h(x) &= \begin{bmatrix} h_1(x) \\ h_2(x) \end{bmatrix} \\ &= \begin{bmatrix} -x_1\sin(\beta_t) + x_2\cos(\beta_t) \\ -x_1\sin(\gamma_t)\cos(\beta_t) - x_2\sin(\gamma_t)\sin(\sigma_t) + x_3\cos(\varepsilon_t) \end{bmatrix} \end{aligned} \tag{8}$$

The goal of CLOS guidance control is to find a control law that reduces tracking error to zero. Specify the vector fields for system (5) X_0 and $X_j, j = 1, 2$ as follows.

$$\begin{cases} X_0 \equiv \dfrac{\partial}{\partial t} + \sum_{o=1}^{8} f_o(x)\dfrac{\partial}{\partial x_0} \\ X_j \equiv \sum_{o=1}^{8} g_{j,o}(x)\dfrac{\partial}{\partial x_0} \end{cases} \tag{9}$$

where $f_o(x)$, $g_{j,o}(x)$, and x_o are the o-th components of $\boldsymbol{f}(x)$, $\boldsymbol{g}(x)$, and x respectively [9]. Direct computation yields

$$\begin{aligned} X_0h_1 &= -\dot{\beta}_t x_1 c\beta_t - \dot{\beta}_t x_2 s\beta_t - x_4 c\beta_t + x_5 c\beta_t \\ &= -\dot{\beta}_t R_p c\varepsilon_t + \dot{\beta}_t e_2 - x_4 c\beta_t + x_5 c\beta_t \\ X_0h_2 &= \left(\dot{\beta}_t \sin(\beta_t)\sin(\varepsilon_t) - \dot{\varepsilon}_t \cos(\varepsilon_t)\cos(\beta_t)\right) x_1 \\ &\quad - \left(\dot{\varepsilon}_t \cos(\varepsilon_t)\sin(\beta_t) + \dot{\beta}_t \cos(\beta_t)\sin(\varepsilon_t)\right) x_2 \\ &\quad - \dot{\varepsilon}_t x_3 \sin(\varepsilon_t) - x_4 \cos(\beta_t)\sin(\varepsilon_t) \\ &\quad - x_5 \sin(\beta_t)\sin(\varepsilon_t) + x_6 \cos(\varepsilon_t) \\ &= -\dot{\beta}_t e_1 \sin(\varepsilon_t) - \dot{\gamma}_t R_p - x_4 \cos(\beta_t)\sin(\varepsilon_t) \\ &\quad - x_5 \sin(\beta_t)\sin(\varepsilon_t) + x_6 \cos(\varepsilon_t) \\ X_1X_0h_2 &= (\cos(\varepsilon_t)\cos(x_8) + \sin(\varepsilon_t)\sin(x_8)\cos(x_7 - \beta_t)) \\ &\quad \times \sin(\phi_{mc}) + \cos(\phi_{mc})\sin(\varepsilon_t)\sin(x_7 - \beta_t) X_2X_oh_2 \\ &= (\cos(\varepsilon_t)\cos(x_8) + \sin(\varepsilon_t)\sin(x_8)\cos(x_7 - \beta_t)) \\ &\quad \times \sin(\phi_{mc}) - \sin(\phi_{mc})\sin(\varepsilon_t)\sin(x_7 - \beta_t) \\ X_1X_0h_1 &= -\sin(\phi_{mc})\sin(x_8)\sin(x_7 - \beta_t) \\ &\quad + \cos(\phi_{mc})\cos(x_7 - \beta_t) \\ X_2X_0h_1 &= -\cos(\phi_{mc})\sin(x_8)\sin(x_7 - \beta_t) \\ &\quad - \sin(\phi_{mc})\cos(x_7 - \beta_t) \\ X_0^2h_1 &= \left(2\dot{\beta}_t\dot{\varepsilon}_t \sin(\varepsilon_t) - \ddot{\beta}_t \cos(\varepsilon_t)\right) R_p + \dot{\beta}_t^2 e_1 \\ &\quad + \left(2\dot{\beta}_t\dot{\gamma}_t \cos(\varepsilon_t) + \ddot{\beta}_t \sin(\varepsilon_m)\right) e_2 \\ &\quad - 2\dot{\beta}_t\dot{R}_p \cos(\varepsilon_t) + 2\dot{\beta}_t\dot{e}_2 \sin(\varepsilon_t) \\ &\quad + a_x(t)\cos(x_8)\sin(x_7 - \beta_t) \end{aligned}$$

$$
\begin{aligned}
X_0^2 h_2 = & -\left(\ddot{\varepsilon}_t + \dot{\beta}_t^2 \sin(\varepsilon_t)\cos(\varepsilon_t)\right) R_p - \ddot{\beta}_t e_1 \sin(\gamma_t) \\
& + \left(\dot{\beta}_t^2 \sin(\varepsilon_t)\sin(\varepsilon_t) + \dot{\varepsilon}\gamma_t^2\right) e_2 \\
& - 2\dot{\varepsilon}_t \dot{R}_p - 2\dot{\beta}_t \dot{e}_1 \sin(\varepsilon_t) \\
& + (\sin(x_8)\cos(\varepsilon_t) - \cos(x_8)\sin(\varepsilon_t)\cos(x_7 - \beta_t)) \\
& \times a_x(t) - g\cos(\varepsilon_t) \\
\dot{R}_p = & -\left(\dot{\beta}_t \sin(\beta_t)\cos(\varepsilon_t) - \dot{\varepsilon}_t \sin(\varepsilon_t)\cos(\beta_t)\right) x_1 \\
& - \left(\dot{\varepsilon}_t \sin(\varepsilon_t)\sin(\beta_t) - \dot{\beta}_t \cos(\beta_t)\cos(\varepsilon_t)\right) x_2 \\
& + \dot{\varepsilon}_t x_3 \cos(\varepsilon_t) + x_4 \cos(\varepsilon_t)\cos(\beta_t) \\
& + x_5 \cos(\varepsilon_t)\sin(\beta_t) + x_6 \sin(\varepsilon_t) \qquad (10)
\end{aligned}
$$

Equation (3) can be expressed in a more compact form by some manipulations:

$$
\boldsymbol{e} = \begin{bmatrix} F_1 \\ F_2 \end{bmatrix} + \begin{bmatrix} G_{11} & G_{12} \\ G_{21} & G_{22} \end{bmatrix} \begin{bmatrix} u_1 \\ u_2 \end{bmatrix} \equiv \boldsymbol{F} + \boldsymbol{G}\boldsymbol{u} \qquad (11)
$$

where $F_1 = X_0^2 h_1$, $F_2 = X_0^2 h_2$, $G_{11} = X_1 X_0 h_1$, $G_{12} = X_2 X_0 h_1$, $G_{21} = X_1 X_o h_2$, and $G_{22} = X_2 X_o h_2$. Choosing a sliding surface as follows.

$$
\boldsymbol{s} \equiv \boldsymbol{e} + \Omega \int_0^t \boldsymbol{e}(\tau) d\tau \qquad (12)
$$

where $\Omega = \begin{bmatrix} \xi_1 & 0 \\ 0 & \xi_2 \end{bmatrix} \in \Re^{2\times 2}$ is a two-dimensional space governed by a positive, diagonal, nonnegative matrix.

$$
\Rightarrow \dot{\boldsymbol{s}} \equiv \dot{\boldsymbol{e}} + \Omega \boldsymbol{e} \qquad (13)
$$

To illustrate, the mathematical model for an ideal controller $\boldsymbol{u}_{\text{ideal}}$ looks like:

$$
\boldsymbol{u}_{\text{ideal}} = \boldsymbol{G}^{-1}(-\boldsymbol{F} - \Omega \boldsymbol{e}) \qquad (14)
$$

Replacing (14) into (11), obtains

$$
\dot{\boldsymbol{e}} + \Omega \times \boldsymbol{e} = 0 \qquad (15)
$$

The choice to represent the coefficients of a Hurwitz polynomial in (12) leads to the conclusion that $\lim_{t\to\infty} \|\boldsymbol{s}\| \to 0 \Rightarrow \lim_{t\to\infty} \|\boldsymbol{e}\| \to 0$. However, it is not possible to obtain the exact model for $\boldsymbol{u}_{\text{ideal}}$ in (14), since models always depend on the flight conditions with strong uncertainties. For this reason, a Takagi-Kang-Sugeno elliptic type-2 fuzzy brain imitated neural network (TSKET2FBINN) controller is proposed to imitate the ideal controller.

III. TSK ELLIPTIC TYPE-2 FUZZY BRAIN IMITATED NEURAL NETWORK

An architecture of the proposed TSKET2FBINN is depicted in figure 3, which consists of five spaces: input space, elliptic type-2 function space, sensory weight space and emotional weight space, amygdala space, orbitofrontal cortex space, and output space. The specifics of TSKET2FBINN can be listed as follows.

A. INPUT SPACE

$\Upsilon = \left[\Upsilon_1, \Upsilon_2, \ldots, \Upsilon_{n_i}\right] \in R^{n_i}$, n_i is the input dimension.

B. ELLIPTIC TYPE-2 FUNCTION SPACE

Lower and upper elliptic type-2 function are respectively described as

$$
\underline{\mu}_{ij}(\Theta_{ij}) = \begin{cases} \left(1 - \Theta_{ij}^{\underline{q}_{ij}}\right)^{\frac{1}{\underline{q}_{ij}}}, & \text{if } \Theta_{ij} < 1 \\ 0, & \text{others} \end{cases} \qquad (16)
$$

$$
\overline{\mu}_{ij}(\Upsilon_i) = \begin{cases} \left(1 - \left|\frac{\Upsilon_i - m_{ij}}{v_{ij}}\right|^{\overline{q}_{ij}}\right)^{\frac{1}{\overline{q}_{ij}}}, & \text{if } \left|\frac{\Upsilon_i - m_{ij}}{v_{ij}}\right| < 1 \\ 0, & \text{others} \end{cases} \qquad (17)
$$

where v_{ij} and m_{ij} are respectively center and dilation of the elliptic type-2 function. Set $\Theta_{ij} = \left|\frac{\Upsilon_i - m_{ij}}{v_{ij}}\right|$, equations (16) and (17) can be rewritten as follows.

$$
\underline{\mu}_{ij}(\Theta_{ij}) = \begin{cases} \left(1 - \Theta_{ij}^{\underline{q}_{ij}}\right)^{\frac{1}{\underline{q}_{ij}}}, & \text{if } \Theta_{ij} < 1 \\ 0, & \text{others} \end{cases} \qquad (18)
$$

$$
\overline{\mu}_{ij}(\Theta_{ij}) = \begin{cases} \left(1 - \Upsilon_{ij}^{\overline{q}_{ij}}\right)^{\frac{1}{\overline{q}_{ij}}}, & \text{if } \Theta_{ij} < 1 \\ 0, & \text{others} \end{cases} \qquad (19)
$$

C. SENSORY WEIGHT SPACE AND EMOTIONAL WEIGHT SPACE

Upper and lower weights of the sensory space are defined as follows by the TSK fuzzy system and the wavelet function of the input.

$$
\overline{V}_{jo} = \sum_{i=1}^{n_i} \left(\frac{-(\Upsilon_i - b_{ij})}{\overline{a}_{ij}}\right) e^{\frac{-(\Upsilon_i - b_{ij})^2}{2\overline{a}_{ij}^2}} \times \omega_{jo} \qquad (20)
$$

Set

$$
\overline{Z}_{ij} = \frac{(\Upsilon_i - b_{ij})}{\overline{a}_{ij}} \qquad (21)
$$

$$
\overline{V}_{jo} = \sum_{i=1}^{n_i} \left(-\overline{Z}_{ij}\right) e^{\frac{-\overline{Z}_{ij}^2}{2}} \times \omega_{jo} \qquad (22)
$$

$$
\underline{V}_{jo} = \sum_{i=1}^{n_i} \left(\frac{-(\Upsilon_i - b_{ij})}{\underline{a}_{ij}}\right) e^{\frac{-(\Upsilon_i - b_{ij})^2}{2\underline{a}_{ij}^2}} \times \omega_{jo} \qquad (23)
$$

$$
\underline{Z}_{ij} = \frac{(\Upsilon_i - b_{ij})}{\underline{a}_{ij}} \qquad (24)
$$

$$
\underline{V}_{io} = \sum_{i=1}^{n_i} \left(-\underline{Z}_{ij}\right) e^{\frac{-\underline{Z}_{ij}^2}{2}} \times \omega_{jo} \qquad (25)
$$

The upper and lower weights of the emotional space are defined using the TSK fuzzy system and the wavelet function.

$$
\overline{W}_{io} = \sum_{i=1}^{n_i} \left(\frac{-(\Upsilon_i - b_{ij})}{\overline{a}_{ij}}\right) e^{\frac{-(\Upsilon_i - b_{ij})^2}{2\overline{a}_{ij}^2}} \times \chi_{jo} \qquad (26)
$$

$$
\underline{W}_{jo} = \sum_{i=1}^{n_i} \left(\frac{-(\Upsilon_i - b_{ij})}{\underline{a}_{ij}}\right) e^{\frac{-(\Upsilon_i - b_{ij})^2}{2\underline{a}_{ij}^2}} \times \chi_{jo} \qquad (27)
$$

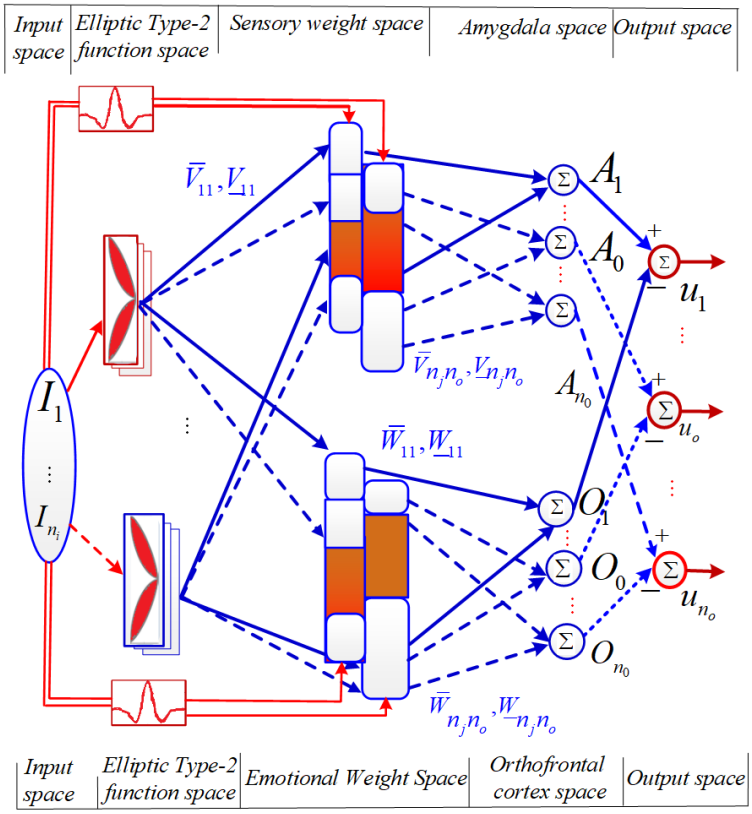

FIGURE 3. The architecture of Takagi-Kang-Sugeno elliptic type-2 fuzzy brain imitated neural network.

where χ_{jo} is a weight

$$\overline{W}_{jo} = \sum_{i=1}^{n_i} \left(-\overline{Z}_{ij}\right) e^{\frac{-\overline{Z}_{ij}^2}{2}} \times \chi_{jo} \tag{28}$$

$$\underline{W}_{jo} = \sum_{i=1}^{n_i} \left(-\underline{Z}_{ij}\right) e^{\frac{-\underline{Z}_{ij}^2}{2}} \times \chi_{jo} \tag{29}$$

D. AMYGDALA AND ORBITOFRONTAL CORTEX SUB-OUTPUT SPACE

$$\begin{aligned}\alpha_o &= \frac{1}{2}\cdot\frac{\sum_{i=1}^{n_i}\sum_{j=1}^{n_j}\underline{\mu}_{ij}\underline{V}_{ijo}}{\sum_{i=1}^{n_i}\sum_{j=1}^{n_j}\underline{\mu}_{ij}} + \frac{1}{2}\cdot\frac{\sum_{i=1}^{n_i}\sum_{j=1}^{n_j}\overline{\mu}_{ij}\overline{V}_{ijo}}{\sum_{i=1}^{n_i}\sum_{j=1}^{n_j}\overline{\mu}_{ij}} \\ &= \frac{1}{2}\cdot\left(\frac{\sum_{i=1}^{n_i}\sum_{j=1}^{n_j}\left(1-F_{ij}^{\overline{q}_{ij}}\right)^{\frac{1}{\overline{q}_{ij}}}\overline{V}_{ijo}}{\sum_{i=1}^{n_i}\sum_{j=1}^{n_j}\left(1-F_{ij}^{\overline{q}_{ij}}\right)^{\frac{1}{\overline{q}_{ij}}}} + \frac{\sum_{i=1}^{n_i}\sum_{j=1}^{n_j}\left(1-F_{ij}^{\underline{q}_{ij}}\right)^{\frac{1}{\underline{q}_{ij}}}\underline{V}_{ijo}}{\sum_{i=1}^{n_i}\sum_{j=1}^{n_j}\left(1-F_{ij}^{\underline{q}_{ij}}\right)^{\frac{1}{\underline{q}_{ij}}}}\right)\end{aligned} \tag{30}$$

$$\begin{aligned}o_o &= \frac{1}{2}\cdot\frac{\sum_{i=1}^{n_i}\sum_{j=1}^{n_j}\underline{\mu}_{ij}\underline{W}_{ijo}}{\sum_{i=1}^{n_i}\sum_{j=1}^{n_j}\underline{\mu}_{ij}} + \frac{1}{2}\cdot\frac{\sum_{i=1}^{n_i}\sum_{j=1}^{n_j}\overline{\mu}_{ij}\overline{W}_{ijo}}{\sum_{i=1}^{n_i}\sum_{j=1}^{n_j}\overline{\mu}_{ij}} \\ &= \frac{1}{2}\cdot\left(\frac{\sum_{i=1}^{n_i}\sum_{j=1}^{n_j}\left(1-\Theta_{ij}\overline{q}_{ij}\right)^{\frac{1}{\overline{q}_{ij}}}\overline{W}_{ijo}}{\sum_{i=1}^{n_j}\sum_{j=1}^{n_j}\left(1-\Theta_{ij}^{\overline{q}_{ij}}\right)^{\frac{1}{\overline{q}_{ij}}}} + \frac{\sum_{i=1}^{n_{ij}}\sum_{j=1}^{n_j}\left(1-\Theta_{ij}\underline{q}_{ij}\right)^{\frac{1}{\underline{q}_{ij}}}\underline{W}_{ijo}}{\sum_{i=1}^{n_i}\sum_{j=1}^{n_j}\left(1-\Theta_{ij}^{\underline{q}_{ij}}\right)^{\frac{1}{\underline{q}_{ij}}}}\right)\end{aligned} \tag{31}$$

E. OUTPUT SPACE

The o-th output of the TSKET2FBINN controller can be calculated as

$$u_{\text{TSKET2FBINN}}^{o} = \alpha_o - o_o \text{ for } o = 1, 2 \ldots, n_o \tag{32}$$

IV. ONLINE LEARNING RULES AND CONVERGENCE ANALYSIS

Selecting a cost function as follows.

$$\Xi = \frac{1}{2}\sum_{o=1}^{n_o} s_o^2 \tag{33}$$

where $s_o = s_o^{\text{desired}} - z_o$ in which s_o^{desired} is the desired output. An expression for the rule governing the periodic updating of parameters is derived as follows.

$$\xi(t+1) = \xi(t) + \Delta\xi \tag{34}$$

where ξ possibly depends on one of these factors $\overline{V}_{ijo}, \underline{V}_{ijo}, \overline{W}_{ijo}, \underline{W}_{ijo}, m_{ij}, v_{ij}, \underline{q}_{ij}$ or $\overline{q}_{ij}$. Instead of updating $\overline{V}, V, \overline{W}$, and W, we will instead update $b, \overline{a}, a, \omega$ and χ. The law for adjusting these parameters are expressed by the chain rule as follows.

$$\begin{aligned}
\Delta m_{ij} &= -\zeta_m . \frac{\partial \Xi}{\partial m_{ij}} \\
&= -\zeta_m \left(\frac{\partial \Xi}{\partial s_o} . \frac{\partial s_o}{\partial z_o} . \frac{\partial z_o}{\partial u_o} . \frac{\partial u_o}{\partial \underline{\mu}_{ij}} . \frac{\partial \underline{\mu}_{ij}}{\partial \Theta_{ij}} . \frac{\partial \Theta_{ij}}{\partial m_{ij}} \right. \\
&\quad \left. + \frac{\partial \Xi}{\partial s_o} . \frac{\partial s_o}{\partial z_o} . \frac{\partial z_o}{\partial u_o} . \frac{\partial u_o}{\partial \overline{\mu}_{ij}} . \frac{\partial \overline{\mu}_{ij}}{\partial \Theta_{ij}} . \frac{\partial \Theta_{ij}}{\partial m_{ij}} \right) \\
&= -\zeta_m . \frac{\partial \Xi}{\partial s_o} . \frac{\partial s_o}{\partial z_o} . \frac{\partial z_o}{\partial u_o} \left(\frac{\partial u_o}{\partial \underline{\mu}_{ij}} . \frac{\partial \underline{\mu}_{ij}}{\partial \Theta_{ij}} \frac{\partial \Theta_{ij}}{\partial m_{ij}} \right. \\
&\quad \left. + \frac{\partial u_o}{\partial \overline{\mu}_{ij}} . \frac{\partial \overline{\mu}_{ij}}{\partial \Theta_{ij}} . \frac{\partial \Theta_{ij}}{\partial m_{ij}} \right)
\end{aligned} \tag{35}$$

$$\frac{\partial \Xi}{\partial s_o} = \sum_{o=1}^{n_o} s_o \tag{36}$$

$$\frac{\partial s_o}{\partial z_o} = -1 \tag{37}$$

$$\frac{\partial z_o}{\partial u_o} = z_o(1 - z_o) \tag{38}$$

$$\frac{\partial u_o}{\partial \underline{\mu}_{ij}} = \underline{V}_{ijo} - \underline{W}_{ijo} \tag{39}$$

$$\frac{\partial u_o}{\partial \overline{\mu}_{ij}} = \overline{V}_{ijo} - \overline{W}_{ijo} \tag{40}$$

where $\zeta_m, \zeta_v, \zeta_q, \zeta_{\overline{q}}, \zeta_b, \zeta_a, \zeta_{\overline{a}}, \zeta_\omega$, and ζ_χ stand for learning rates.

The proposed TSKET2FBINN-based control system for missile guidance is proposed to minimize tracking error. The proposed control system includes a TSKET2FBINN controller $\boldsymbol{u}_{\text{TSKET2FBINN}}$ and a robust compensator $\boldsymbol{u}_{RC}$, as shown in Fig. 4, The $\boldsymbol{u}_{\text{TSKET2FBINN}}$ serves as the main controller, while the robust compensator $\boldsymbol{u}_{RC}$ compensates for any discrepancies and guarantees system stability.

Robust compensator control system design

From the nature of the approximation error between the TSKET2FBINN and the ideal controller, the following can be deduced about the overall control system for the proposed TSKET2FBINN:

$$\boldsymbol{u}_{\text{ideal}} = \boldsymbol{u}_{\text{TSKET2FBINN}} + \boldsymbol{\varepsilon} \tag{59}$$

where $\boldsymbol{\varepsilon} = [\varepsilon_1, \varepsilon_2, \ldots, \varepsilon_{n_o}]^T \in \Re^{n_o}$ stands for the vector of approximation errors.

To mitigate the potential for approximation error in (59), we use an H∞ tracking power [26] in the following way:

$$\sum_{o=1}^{n_o} \int_0^T s_o^2 dt \le \sum_{i=1}^{m} \int_0^T s_o^2(0) + \sum_{i=1}^{m} \beta_o^2 \left(\int_0^T \varepsilon_o^2 dt \right) \tag{60}$$

With all initial conditions setting to zero, (60) simplifies to

$$\sup_{\varepsilon_o \in L_2[0,T]} \frac{\|s_o\|}{\|\varepsilon_o\|} \le \beta_o \tag{61}$$

where $\|s_o\|^2 = \int_0^T s_o^2 dt$ and $\|s_o\|^2 = \int_0^T s_o^2 . dt$.

From this, it can be seen that robustness can be improved by choosing an appropriate attenuation level β_o [31]. Then a theorem is expressed as follows:

Theorem 1: The missile guidance system described in equation (1). The $\boldsymbol{u}_{TSKET2FBINN}$ is proposed in equation (32), the online parameter learning algorithms of TSKET2FBINN are presented in equations (35)-(58), and the robust compensator is formulated as

$$\boldsymbol{u}_{\text{RC}} = \frac{1}{2}(\beta^T \beta)^{-1}(\beta^T \beta + \boldsymbol{I}).\boldsymbol{s}(t) \tag{62}$$

where $\beta = diag(\beta_1, \beta_2, \ldots, \beta_{n_o}) \in \Re^{n_o \times n_o}$ is a square matrix, $\boldsymbol{I} = diag(1, 1, \ldots, 1) \in \Re^{n_o \times n_o}$, and $\boldsymbol{s} = [s_1 s_2 \ldots s_{n_o}]^T \in \Re^{n_o}$. The system can be stable and robust.

Proof: The following is a definition of the Lyapunov function.

$$\boldsymbol{V}_2 = \frac{\boldsymbol{s}^T \boldsymbol{s}}{2} = \frac{1}{2} \sum_{o=1}^{n_o} s_o^2 \tag{63}$$

The derivative of (63) is calculated as follows.

$$\begin{aligned}
\dot{\boldsymbol{V}}_2 &= \boldsymbol{s}^T \dot{\boldsymbol{s}} = \boldsymbol{e}^T \left(\boldsymbol{\varepsilon} - \frac{1}{2}(\beta^T \beta)^{-1}(\boldsymbol{\beta}^T \beta + \boldsymbol{I}).\boldsymbol{s}(t) \right) \\
\dot{\boldsymbol{V}}_2 &= \sum_{i=o}^{n_o} \left(-s_o \varepsilon_o - \frac{s_o^2}{2} - \frac{s_o^2}{2\beta_o^2} \right) \\
&= \sum_{o=1}^{n_o} \left(\frac{-e_o^2}{2} - \frac{1}{2} \left(\frac{e_o}{\beta_o} + \beta_o \varepsilon_o \right)^2 + \frac{\beta_o^2 \varepsilon_o^2}{2} \right) \\
&\le \sum_{o=1}^{n_o} \left(\frac{-e_o^2}{2} + \frac{\beta_o^2 \varepsilon_o^2}{2} \right)
\end{aligned} \tag{64}$$

where $\varepsilon_o(t) \in \boldsymbol{L}_2[0, T], \forall T \in [0, \infty)$. When the preceding equation is integrated, the result is:

$$\boldsymbol{V}_2(T) - \boldsymbol{V}_2(0) \le \sum_{o=1}^{n_o} \left(-\int_0^T \frac{s_o^2}{2} dt + \frac{\beta_o^2}{2} \int_0^T \varepsilon_o^2 dt \right) \tag{65}$$

Meanwhile $\boldsymbol{V}_2(T) \ge 0$, The following inequality can be deduced from the previous inequality.

$$\frac{1}{2} \sum_{o=1}^{n_o} \int_0^T s_o^2 dt \le \left(\boldsymbol{V}(0) + \frac{\beta_o^2}{2} \sum_{o=1}^{n_o} \left(\int_0^T \varepsilon_o^2 dt \right) \right) \tag{66}$$

$$\frac{\partial \underline{\mu}_{ij}}{\partial \Theta_{ij}}.\frac{\partial \Theta_{ij}}{\partial m_{ij}} = \frac{-1}{|v_{ij}|}\text{sign}(\Upsilon_i - m_{ij})\left|\frac{\Upsilon_i - m_{ij}}{v_{ij}}\right|^{\left(\underline{q}_{ij}-1\right)} \times \left(1 - \left|\frac{\Upsilon_i - m_{ij}}{v_{ij}}\right|^{\underline{q}_{ij}}\right)^{\left(\frac{1}{\underline{q}_{ij}}-1\right)}$$
$$= \frac{-1}{|v_{ij}|}\text{sign}(\Upsilon_i - m_{ij})\Upsilon_{ij}^{\underline{q}_{ij}-1} \times \left(1 - \Upsilon_{ij}^{\underline{q}_{ij}}\right)^{\left(\frac{1}{\underline{q}_{ij}}-1\right)} \tag{41}$$

$$\frac{\partial \overline{\mu}_{ij}}{\partial \Theta_{ij}}.\frac{\partial \Theta_{ij}}{\partial m_{ij}} = \frac{-1}{|v_{ij}|}.\text{sign}(\Upsilon_i - m_{ij})\left|\frac{\Upsilon_i - m_{ij}}{v_{ij}}\right|^{(\overline{q}_{ij}-1)} \times \left(1 - \left|\frac{\Upsilon_i - m_{ij}}{v_{ij}}\right|^{\overline{q}_{ij}}\right)^{\left(\frac{1}{\overline{q}_{ij}}-1\right)}$$
$$= \frac{-1}{|v_{ijk}|}\text{sign}(\Upsilon_i - m_{ij})\Theta_{ij}^{\overline{q}_{ijk}-1} \times \left(1 - \Theta_{ij}^{\overline{q}_{ij}}\right)^{\left(\frac{1}{\overline{q}_{ij}}-1\right)} \tag{42}$$

$$\Delta m_{ij} = \zeta_m \sum_{o=1}^{n_o} s_o z_o (1 - z_o) \times \left(-\frac{(\underline{V}_{ijo} - \underline{W}_{ijo})}{|v_{ij}|}\text{sign}(\Upsilon_i - m_{ij})\Theta_{ij}^{\underline{q}_{ij}-1} \times \left(1 - \Theta_{ij}^{\underline{q}_{ij}}\right)^{\left(\frac{1}{\underline{q}_{ij}}-1\right)} \right.$$
$$\left. -\frac{(\overline{V}_{ijo} - \overline{W}_{ijo})}{|v_{ij}|}\text{sign}(\Upsilon_i - m_{ij})\Theta_{ij}^{\overline{q}_{ij}-1} \times \left(1 - \Theta_{ij}^{\overline{q}_{ij}}\right)^{\left(\frac{1}{\overline{q}_{ij}}-1\right)} \right) \tag{43}$$

$$\Delta v_{ij} = -\zeta_v.\frac{\partial \Xi}{\partial v_{ij}} = -\zeta_v \left(\frac{\partial \Xi}{\partial s_o}.\frac{\partial s_o}{\partial z_o}.\frac{\partial z_o}{\partial u_o}.\frac{\partial u_o}{\partial \underline{\mu}_{ij}}.\frac{\partial \underline{\mu}_{ij}}{\partial \Theta_{ij}}.\frac{\partial \Theta_{ij}}{\partial v_{ij}} + \frac{\partial \Xi(k)}{\partial s_o}.\frac{\partial s_o}{\partial z_o}.\frac{\partial z_o}{\partial u_o}.\frac{\partial u_o}{\partial \overline{\mu}_{ij}}.\frac{\partial \overline{\mu}_{ij}}{\partial \Theta_{ij}}.\frac{\partial \Theta_{ij}}{\partial v_{ij}} \right)$$
$$= -\zeta_v \frac{\partial \Xi}{\partial s_o}.\frac{\partial s_o}{\partial z_o}.\frac{\partial z_o}{\partial u_o}\left(\frac{\partial u_o}{\partial \underline{\mu}_{ij}}.\frac{\partial \underline{\mu}_{ij}}{\partial v_{ij}} + \frac{\partial u_o}{\partial \overline{\mu}_{ij}}.\frac{\partial \overline{\mu}_{ij}}{\partial v_{ij}} \right) \tag{44}$$

$$\frac{\partial \underline{\mu}_{ij}}{\partial v_{ij}} = \frac{-1}{|v_{ijk}|^2}\text{sign}\,|v_{ijk}|\,|\Upsilon_i - m_{ijk}|\left|\frac{\Upsilon_i - m_{ijk}}{v_{ijk}}\right|^{\left(\underline{q}_{ijk}-1\right)} \times \left(1 - \left|\frac{\Upsilon_i - m_{ijk}}{v_{ijk}}\right|^{\underline{q}_{ijk}}\right)^{\left(\frac{1}{\underline{q}_{ijk}}-1\right)}$$
$$= \frac{-1}{|v_{ijk}|^2}\text{sign}\,|v_{ijk}|\,|\Upsilon_i - m_{ijk}|\,\Theta_{ij}^{\underline{q}_{ijk}-1} \times \left(1 - \Theta_{ij}^{\underline{q}_{ij}}\right)^{\left(\frac{1}{\underline{q}_{ijk}}-1\right)} \tag{45}$$

$$\frac{\partial \overline{\mu}_{ijk}}{\partial v_{ijk}} = \frac{-\text{sign}\,|v_{ijk}|}{|v_{ijk}|^2}.|I_i - m_{ijk}|.\left|\frac{I_i - m_{ijk}}{v_{ijk}}\right|^{(\overline{q}_{ijk}-1)} \times \left(1 - \left|\frac{I_i - m_{ijk}}{v_{ijk}}\right|^{\overline{q}_{ijk}}\right)^{\left(\frac{1}{\overline{q}_{ijk}}-1\right)}$$
$$= \frac{-\text{sign}\,|v_{ijk}|}{|v_{ijk}|^2}\,|\Upsilon_i - m_{ijk}|.\Theta_{ij}^{\overline{q}_{ijk}-1}\left(1 - \Theta_{ij}^{\overline{q}_{ijk}}\right)^{\left(\frac{1}{\overline{q}_{ijk}}-1\right)} \tag{46}$$

$$\Delta v_{ij} = -\zeta_v \sum_{o=1}^{n_o} s_o z_o (1 - z_o) \times \left(-\frac{(\underline{V}_{ijo} - \underline{W}_{ijo})}{|v_{ijk}|^2}\text{sign}\,|v_{ijk}|\,|\Upsilon_i - m_{ijk}|.\Theta_{ij}^{\underline{q}_{ijk}-1}\left(1 - \Theta_{ij}^{\underline{q}_{ij}}\right)^{\left(\frac{1}{\underline{q}_{ijk}}-1\right)} \right.$$
$$\left. -\frac{(\overline{V}_{ijo} - \overline{W}_{ijo})}{|v_{ijk}|^2}\text{sign}\,|v_{ijk}|\,|\Upsilon_i - m_{ijk}|\,\Theta_{ij}^{\overline{q}_{ijk}-1}\left(1 - \Theta_{ij}^{\overline{q}_{ijk}}\right)^{\left(\frac{1}{\overline{q}_{ijk}}-1\right)} \right) \tag{47}$$

$$\Delta \underline{q}_{ij} = -\zeta_q \frac{\partial \Xi}{\partial \underline{q}_{ij}} = -\zeta_q \frac{\partial \Xi}{\partial s_o}.\frac{\partial s_o}{\partial z_o}.\frac{\partial z_o}{\partial u_o}.\frac{\partial u_o}{\partial \underline{\mu}_{ij}}.\frac{\partial \underline{\mu}_{ij}}{\partial \underline{q}_{ij}} \tag{48}$$

$$\frac{\partial \underline{\mu}_{ij}}{\partial \underline{q}_{ij}} = \frac{1}{\underline{q}_{ijk}^2}\ln\left(1 - \Theta_{ij}^{\underline{q}_{ij}}\right)\left(1 - \Theta_{ij}^{\underline{q}_{ij}}\right)^{\frac{1}{\underline{q}_{ijk}}} - \frac{1}{\underline{q}_{ijk}}\ln(\Theta_{ij}).\Theta_{ij}^{\underline{q}_{ij}}\left(1 - \Theta_{ij}^{\underline{q}_{ij}}\right)^{\left(\frac{1}{\underline{q}_{ijk}}-1\right)} \tag{49}$$

$$\Delta \underline{q}_{ij} = -\zeta_q \sum_{o=1}^{n_o} s_o.z_o.(1 - z_o)(\underline{V}_{ijo} - \underline{W}_{ijo})\left(\frac{1}{\underline{q}_{ijk}^2}\ln\left(1 - \Theta_{ij}^{\underline{q}_{ij}}\right)\left(1 - \Theta_{ij}^{\underline{q}_{ij}}\right)^{\frac{1}{\underline{q}_{ijk}}} - \frac{1}{\underline{q}_{ijk}}\ln(F_{ij})F_{ij}^{\underline{q}_{ij}}\left(1 - F_{ij}^{\underline{q}_{ij}}\right)^{\left(\frac{1}{\underline{q}_{ijk}}-1\right)} \right) \tag{50}$$

If the initial condition of the system $\boldsymbol{V}(0) = 0$ is satisfied, the following inequality holds:

$$\sup_{\varepsilon_o \in L_2[0,\mathrm{T}]} \sum_{o=1}^{n_o} \int_0^T \frac{\|s_o\|}{\|\varepsilon_o\|} \leq \beta_o \tag{67}$$

where $\|s_o\|^2 = \int_0^T s_o^2 dt$ and $\|\varepsilon_o\|^2 = \int_0^T \varepsilon_o^2 dt$. Based on the desired attenuation ratio, the designer will choose a constant β_o between $\|s_o\|$ and $\|\varepsilon_o\|$ [31], [32]. The robust tracking performance desired by (61) can be achieved with an attenuation level $\boldsymbol{\beta}$. This implies that our proposed method will guarantee the robust stability of the control system.

Remark 1: Regarding the Lyapunov function, the principle for constructing Lyapunov function (63) is that Lyapunov function $\boldsymbol{V}_2$ is dependent on the errors $\boldsymbol{s} = [s_1 s_2 \dots s_{n_o}]^T \in \Re^{n_o}$. It will guarantee that when the Lyapunov function is declined to zero, the error $\boldsymbol{s} = [s_1 s_2 \dots s_{n_o}]^T$ will approach to zero too.

For selecting Lypunov function, for different system and for the different purpose, the Lyapunov function may be selected differently and of course, choosing Lyapunov function will affect to the performance of the system [33]. In this paper, it is seen that the laws for updating the weights of the neural network in equations (35)-(58) depend on the errors $\boldsymbol{s} = [s_1 s_2 \dots s_{n_o}]^T$, therefore, the different Lyapunov function may be influence to the updating of the weights of the neural network. However, in this paper, authors have not yet studied how the Lyapunov function affects to the weight updating process, please allow us study in the future work.

$$\Delta \overline{q}_{ij} = -\zeta_{\overline{q}} \frac{\partial \Xi}{\partial \overline{q}_{ij}} = -\zeta_{\overline{q}} \frac{\partial \Xi}{\partial s_o} \cdot \frac{\partial s_o}{\partial z_o} \cdot \frac{\partial z_o}{\partial u_o} \cdot \frac{\partial u_o}{\partial \overline{\mu}_{ij}} \cdot \frac{\partial \overline{\mu}_{ij}}{\partial \overline{q}_{ij}} \tag{51}$$

$$\frac{\partial \overline{\mu}_{ijk}}{\partial \overline{q}_{ijk}} = \frac{1}{\overline{q}_{ijk}^2} \ln\left(1 - \Theta_{ij}^{\overline{q}_{ij}}\right)\left(1 - \Theta_{ij}^{\overline{q}_{ij}}\right)^{\frac{1}{\overline{q}_{ijk}}} - \frac{1}{\overline{q}_{ijk}} \ln(F_{ij}) F_{ij}^{\overline{q}_{ij}} \times \left(1 - F_{ij}^{\overline{q}_{ij}}\right)^{\left(\frac{1}{\overline{q}_{ijk}} - 1\right)} \tag{52}$$

$$\Delta \overline{q}_{ij} = -\zeta_{\overline{q}} \sum_{o=1}^{n_o} s_o z_o (1 - z_o)(\overline{V}_{ijo} - \overline{W}_{ijo}) \left(\frac{1}{\overline{q}_{ijk}^2} \ln\left(1 - \Theta_{ij}^{\overline{q}_{ij}}\right)\left(1 - \Theta_{ij}^{\overline{q}_{ij}}\right)^{\frac{1}{\overline{q}_{ijk}}} - \frac{\ln(\Theta_{ij})}{\underline{q}_{ijk}} . \Theta_{ij}^{\underline{q}_{ij}} \left(1 - \Theta_{ij}^{\underline{q}_{ij}}\right)^{\left(\frac{1 - \underline{q}_{ijk}}{\underline{q}_{ijk}}\right)} \right) \tag{53}$$

$$\begin{aligned} \Delta b_{ij} &= -\zeta_b \frac{\partial \Xi}{\partial b_{ij}} = -\zeta_b \frac{\partial \Xi}{\partial z_o} \cdot \frac{\partial z_o}{\partial u_o} \cdot \frac{\partial u_o}{\partial \alpha_o} \left(\frac{\partial \alpha_o}{\partial \overline{V}_{ijo}} \cdot \frac{\partial \overline{V}_{ijo}}{\partial \overline{Z}_{ij}} \cdot \frac{\partial \overline{Z}_{ij}}{\partial b_{ij}} + \frac{\partial \alpha_o}{\partial \underline{V}_{ijo}} \cdot \frac{\partial \underline{V}_{ijo}}{\partial \underline{Z}_{ij}} \cdot \frac{\partial \underline{Z}_{ij}}{\partial b_{ij}} \right) \\ &= \frac{-\zeta_b}{2} \sum_{o=1}^{n_o} s_o z_o (1 - z_o) \left(\frac{(\overline{Z}_{ij}^2 - 1)}{\overline{a}_{ij}} e^{\frac{-\overline{Z}_{ij}^2}{2}} + \frac{(\underline{Z}_{ij}^2 - 1)}{\underline{a}_{ij}} e^{\frac{-\underline{Z}_{ij}^2}{2}} \right) \times \omega_{jo} \end{aligned} \tag{54}$$

$$\begin{aligned} \Delta \underline{a}_{ij} &= -\lambda_a \frac{\partial \Xi}{\partial \underline{a}_{ij}} = -\zeta_a \frac{\partial \Xi}{\partial z_o} \cdot \frac{\partial z_o}{\partial u_o} \cdot \frac{\partial u_o}{\partial \alpha_o} \cdot \frac{\partial \alpha_o}{\partial \underline{V}_{ijo}} \cdot \frac{\partial \underline{V}_{ijo}}{\partial \underline{Z}_{ij}} \cdot \frac{\partial \underline{Z}_{ij}}{\partial \underline{a}_{ij}} = -\zeta_a \sum_{o=1}^{n_o} s_o z_o (1 - z_o) \frac{(\underline{Z}_{ij}^2 - 1)}{2} e^{\left(\frac{-\underline{Z}_{ij}^2}{2}\right)} \omega_{jo} \frac{(\Upsilon_i - b_{ij})}{\underline{a}_{ij}^2} \\ &= \frac{-\zeta_a}{2} \sum_{o=1}^{n_o} s_o z_o (1 - z_o)(\underline{Z}_{ij}^2 - 1) e^{\left(\frac{-\underline{Z}_{ij}^2}{2}\right)} \left(\frac{\Upsilon_i - b_{ij}}{\underline{a}_{ij}^2} \right) \omega_{jo} \end{aligned} \tag{55}$$

$$\begin{aligned} \Delta \overline{a}_{ij} &= -\zeta_{\overline{a}} \frac{\partial \Xi}{\partial \overline{a}_{ij}} = -\zeta_{\overline{a}} \frac{\partial \Xi}{\partial z_o} \cdot \frac{\partial z_o}{\partial u_o} \cdot \frac{\partial u_o}{\partial A_o} \cdot \frac{\partial A_o}{\partial \overline{V}_{ijo}} \cdot \frac{\partial \overline{V}_{ijo}}{\partial \overline{Z}_{ij}} \cdot \frac{\partial \overline{Z}_{ij}}{\partial \overline{a}_{ij}} = -\zeta_{\overline{a}} \sum_{o=1}^{n_o} s_o z_o (1 - z_o) \frac{(\overline{Z}_{ij}^2 - 1)}{2} e^{\frac{-\overline{Z}_{ij}^2}{2}} \omega_{jo} \left(\frac{\Upsilon_i - b_{ij}}{\overline{a}_{ij}^2} \right) \\ &= -\frac{\zeta_{\overline{a}}}{2} \sum_{o=1}^{n_o} s_o z_o (1 - z_o)(\underline{Z}_{ij}^2 - 1) e^{\frac{-\underline{Z}_{ij}^2}{2}} \left(\frac{\Upsilon_i - b_{ij}}{\overline{a}_{ij}^2} \right) \omega_{jo} \end{aligned} \tag{56}$$

$$\begin{aligned} \Delta \omega_{jo} &= -\zeta_\omega \frac{\partial \Xi}{\partial \omega_{jo}} = -\zeta_\omega \frac{\partial \Xi}{\partial z_o} \cdot \frac{\partial z_o}{\partial u_o} \cdot \frac{\partial u_o}{\partial \alpha_o} \left(\frac{\partial \alpha_o}{\partial \overline{V}_{ijo}} \cdot \frac{\partial \overline{V}_{ijo}}{\partial \omega_{jo}} + \frac{\partial \alpha_o}{\partial \underline{V}_{ijo}} \cdot \frac{\partial \underline{V}_{ijo}}{\partial \omega_{jo}} \right) = -\zeta_\omega \sum_{o=1}^{n_o} s_o z_o (1 - z_o) \frac{1}{2} \left(\sum_{i=1}^{n_i} \overline{Z}_{ij} e^{\frac{-\overline{Z}_{ij}^2}{2}} + \sum_{i=1}^{n_i} \underline{Z}_{ij} e^{\frac{-\underline{Z}_{ij}^2}{2}} \right) \\ &= \frac{-\zeta_\omega}{2} \sum_{o=1}^{n_o} s_o . z_o (1 - z_o) \left(\sum_{i=1}^{n_i} \overline{Z}_{ij} e^{\frac{-\overline{Z}_{ij}^2}{2}} + \sum_{i=1}^{n_i} \underline{Z}_{ij} e^{\frac{-\underline{Z}_{ij}^2}{2}} \right) \end{aligned} \tag{57}$$

$$\begin{aligned} \Delta \chi_{jo} &= -\zeta_\chi \frac{\partial \Xi}{\partial \chi_{jo}} = -\zeta_\chi \frac{\partial \Xi}{\partial z_o} \cdot \frac{\partial z_o}{\partial u_o} \cdot \frac{\partial u_o}{\partial o_o} \left(\frac{\partial o_o}{\partial \underline{W}_{ijo}} \cdot \frac{\partial \underline{W}_{ijo}}{\partial \chi_{jo}} + \frac{\partial o_o}{\partial \overline{W}_{ijo}} \cdot \frac{\partial \overline{W}_{ijo}}{\partial \chi_{jo}} \right) = \frac{\zeta_\chi}{2} \sum_{o=1}^{n_o} e_o z_o (1 - z_o) \sum_{i=1}^{n_i} (-\overline{Z}_{ij} e^{\left(\frac{-\overline{Z}_{ij}^2}{2}\right)} - \underline{Z}_{ij} e^{\left(\frac{-\underline{Z}_{ij}^2}{2}\right)}) \\ &= \frac{-\zeta_\chi}{2} \sum_{o=1}^{n_o} s_o z_o (1 - z_o) \sum_{i=1}^{n_i} (\overline{Z}_{ij} e^{\frac{-\overline{Z}_{ij}^2}{2}} + \underline{Z}_{ij} e^{\frac{-\underline{Z}_{ij}^2}{2}}) \end{aligned} \tag{58}$$

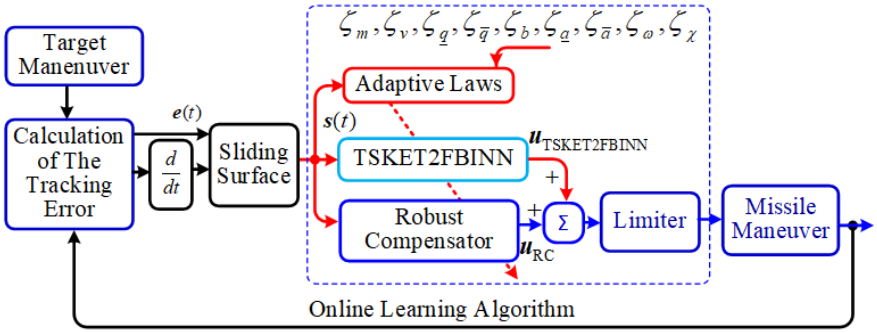

FIGURE 4. The schematic illustration of the proposed control system.

V. SIMULATON RESULTS OF OUR METHOD FOR MISSILE GUIDANCE LAW

We demonstrate the effectiveness of the proposed adaptive guidance law based on TSKET2FBINN using computational simulations. In a closed-loop engagement scenario, it is impossible to evaluate performance characteristics until the target dynamics have been specified. The intended motion model is unlikely to generate any axial acceleration or roll motion. The inertial frame can then be used to represent the simplified dynamics of the target's motion, as demonstrated in [1], [2], and [3].

$$\begin{aligned}
\ddot{x}_t &= -a_{ty}\sin(\psi_t) - a_{tz}\sin(\psi_t)\cos(\theta_t) \\
\ddot{y}_t &= a_{ty}\cos(\psi_t) - a_{tz}\sin(\psi_t)\sin(\theta_t) \\
\ddot{z}_t &= -a_{tz}\cos(\theta_t) - g \\
\dot{\psi}_t &= \frac{a_{ty}}{v_t\cos(\theta_t)} \\
\dot{\theta}_t &= \frac{a_{tz} - g\cos(\theta_t)}{v_t}
\end{aligned} \tag{68}$$

where a_{ty}, a_{tz} are respectively yaw acceleration of target, pitch acceleration of target; θ_t, ψ_t, v_t are respectively pitch angle of target, yaw angle of target, and target velocity.

Remark 2: It is important to note that the missile model in (1) and the target model in (68) are only used for simulation purposes and are not required for the derivation of adaptive TSKET2FBINN-based guidance law. Three different simulation scenarios are examined to demonstrate the viability of the proposed design strategy. Consider the first case (scenario 1), in which the threat originates from the axis, to illustrate an anti-aircraft scenario. The second scenario (scenario 2) is also an anti-aircraft scenario, in which the enemy aircraft approaches from the axis. The final scenario (scenario 3) is a simplified anti-intercontinental-ballistic-missile scenario.

A. SCENARIO 1

The initial of target can be listed in Table 2. The initial values for each parameter of the proposed method are shown in Table 3. Fig. 5 depicts a three-dimensional (3D) missile tracking using our method, Fig. 6 depicts error signals of missile guidance control using our method, Fig. 7 depicts control signals of missile guidance control using our method, and Fig. 8 depicts the miss distance in scenario 1 using our method.

TABLE 2. Initial Parameters of Target and Missile for scenario 1.

	Position [m]	velocity [m/s]
Target parameters	$x_t(0) = 2500$, $y_t(0) = 5361.9$, $z_t(0) = 1000$	$\dot{x}_t(0) = -340$, $\dot{y}_t(0) = 0$, $\dot{z}_t(0) = 0$
$t = 0 \div 2.5$ [s]: $a_{tx} = 5g$, $a_{tz} = -g$; $t > 2.5$ [s]: $a_{ty} = -5g$, $a_{tz} = 5g$		
	Position [m]	**velocity [m/s]**
Missle parameters	$x_m(0) = 14.32$, $y_m(0) = 39.34$, $z_m(0) = 3.36$	$\dot{x}_m(0) = 70.84$, $\dot{y}_m(0) = 151.92$, $\dot{z}_m(0) = 28.32$
$t = 0 \div 2$ [s]: $a_x = 340$ [m/s^2]; $t > 2$ [s]: $a_x = -44.1$ [m/s^2]		

TABLE 3. Initial parameters of the proposed method.

Parameters	Values
Input dimension n_i and Output dimension n_o	8 and 8
Initial value for m_{ij}	0.01
Initial value for v_{ij}	0.8
Initial value for $\underline{q}_{ij}$ and $\overline{q}_{ij}$	0.8 and 1
Initial value for b	0.01
Initial value for $\underline{a}$ and $\overline{a}$	0.005 and 0.008
Initial range for ω	[−0.1, 0.1]
Initial range for χ	[−0.1, 0.1]
Learning-rate for ζ_m, ζ_v, $\zeta_{\underline{q}}$, $\zeta_{\overline{q}}$, ζ_b, $\zeta_{\underline{a}}$, $\zeta_{\overline{a}}$, ζ_ω and ζ_χ	0.00001
Initial value for coefficient β_i $(i=1,2,...,n_i)$ of robust compensator controller	0.5

B. SCENARIO 2

The initial of target and missilecan be listed in Table 4 and the initial values of proposed controller is shown in Table 3.

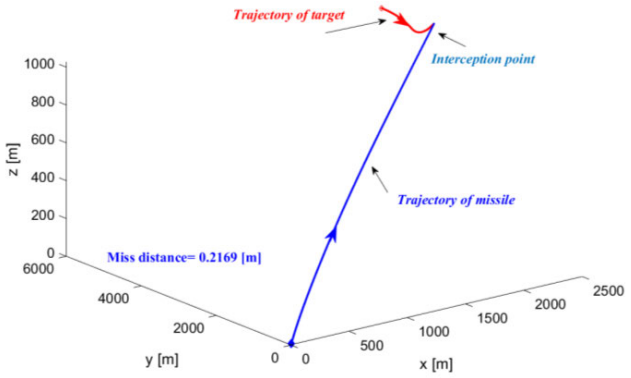

FIGURE 5. Three dimensional (3D) missile tracking with the proposed method.

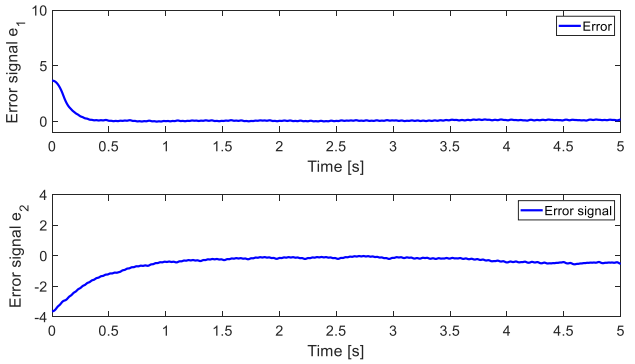

FIGURE 6. Error signals of missile guidance control with the proposed method.

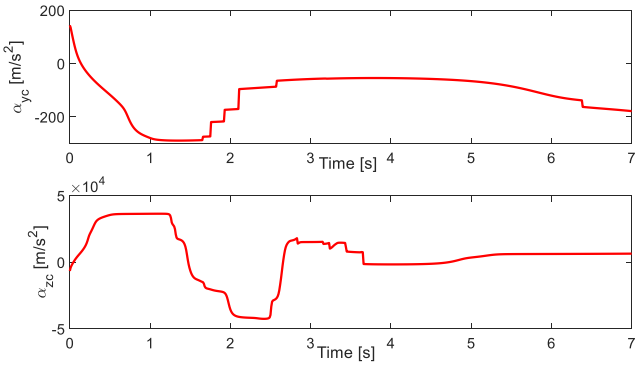

FIGURE 7. Control signals of missile guidance control with the proposed method.

Figure 9 shows the 3D path of the missile in scenario 2 using our method, Figure 10 shows the error signals of the missile, Figure 11 shows the control signals of the missile, and Figure 12 shows the miss distance in scenario 2 using our method.

C. SCENARIO 3

Table 5 lists the initial parameters of the target and the missile. Table 3 also displays the initial values of the proposed controller. Figure 13 depicts the missile's three-dimensional trajectory when our method is applied to the third scenario; Figure 14 depicts the error signals generated by the missile; Figure 15 depicts the control signals generated by the missile; and Figure 16 depicts the distance by which the missile missed its target.

Remark 3: Miss-distance (MD) comparisons between our method and previous methods are presented in Table 6. In scenario 1, the MD of our method is 20.53 times less than the MD

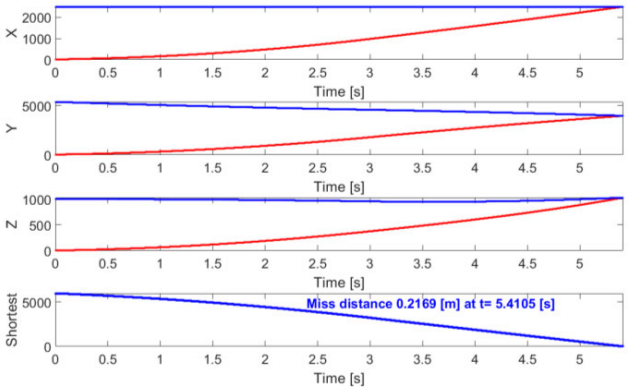

FIGURE 8. Miss distance in scenario 1 using our method.

TABLE 4. Initial parameters of target and missile for scenario 1.

	Position [*m*]	velocity [*m/s*]
Target parameters	$x_t(0)=5200$, $y_t(0)=400$, $z_t(0)=3000$	$\dot{x}_t(0)=340$ $\dot{y}_t(0)=0$ $\dot{z}_t(0)=0$
$t=0\div2.5$ [s]: $a_{tx}=-5g$, $a_{tz}=-g$; $t>2.5$ [s]: $a_{ty}=5g$, $a_{tz}=5g$		
	Position [*m*]	**velocity [*m/s*]**
Missle parameters	$x_m(0)=14.65$ $y_m(0)=5.43$ $z_m(0)=10.01$	$\dot{x}_t(0)=129.65$ $\dot{y}_t(0)=12.87$ $\dot{z}_t(0)=92.42$
$t=0\div2$ [s]: $a_x=340$ [m/s^2]; $t>2$ [s]: $a_x=44.1$ [m/s^2]		

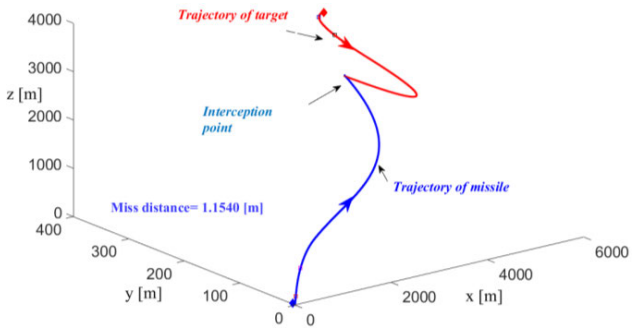

FIGURE 9. 3D trajectory of missile guidance control in scenario 2 using our method.

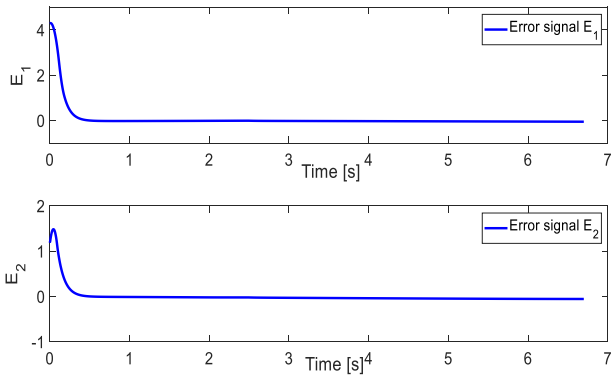

FIGURE 10. Error signals of missile guidance control with the proposed method.

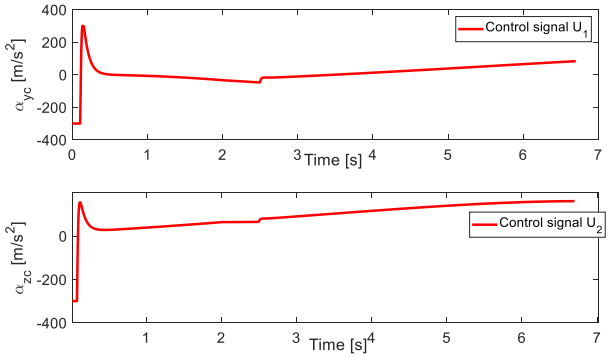

FIGURE 11. Control signals of missile guidance control with the proposed method.

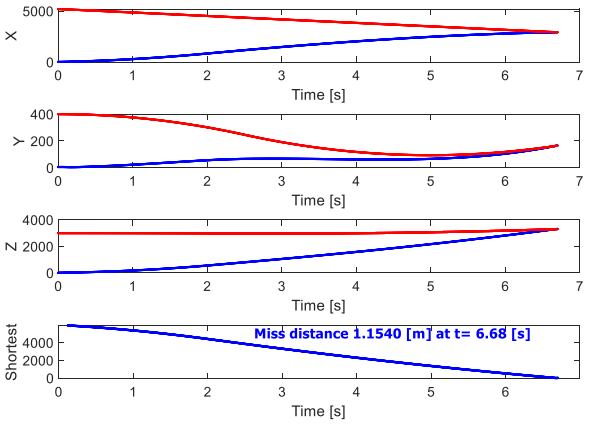

FIGURE 12. Miss distance in scenario 2 using our method.

TABLE 5. Initial parameters of target and missile for scenario 3.

	Position [m]	velocity [m/s]
Target parameters	$x_t(0)=5000$, $y_t(0)=5000$, $z_t(0)=12000$	$\dot{x}_t(0)=0$, $\dot{y}_t(0)=0$, $\dot{z}_t(0)=-500$
$t=0\div7$ [s]: $a_{tx}=-5g$, $a_{tz}=-g$; $t>2.5$ [s]: $a_{ty}=0.5g$, $a_{tz}=-g$		
Missle parameters	Position [m]	velocity [m/s]
	$x_m(0)=28.21$, $y_m(0)=34.81$, $z_m(0)=26.52$	$\dot{x}_t(0)=250$, $\dot{y}_t(0)=250$, $\dot{z}_t(0)=400$
$t=0\div7$ [s]: $a_x=100$ [m/s^2]; $t>7$ [s]: $a_x=-44.1$ [m/s^2]		

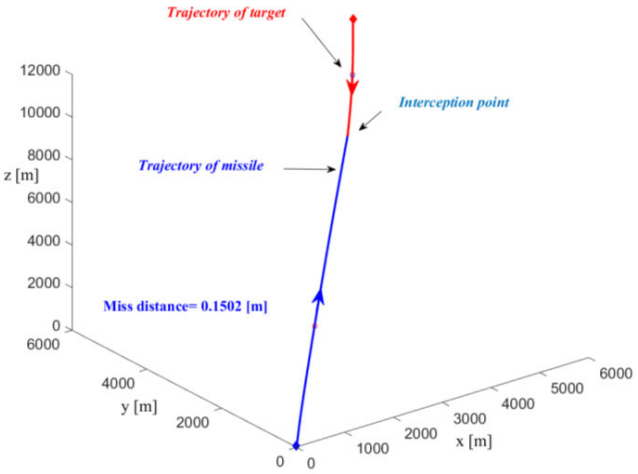

FIGURE 13. 3D pursuit trajectory using our method.

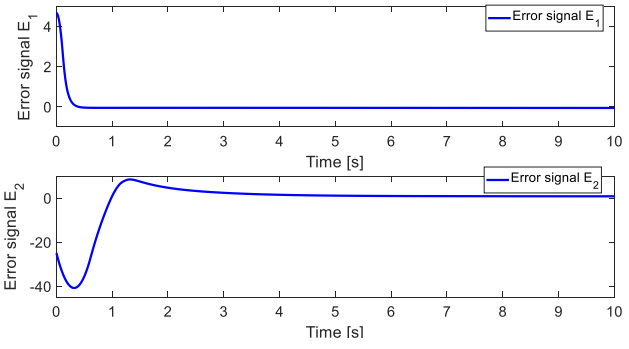

FIGURE 14. Error signals of missile guidance control with our method.

of feedback linerizarion guidance law (FBL) [1], 1.73 times less than the MD of Adaptive CMAC-based guidance law [1], and 1.50 times less than the MD of Adaptive FBELC-based guidance law [1]. In scenario 2, the MD of our method is 2.91 times less than the MD of FBL, 1.16 times less than the MD of CMAC-based guidance law, and 1.10 times less than the MD of FBELC-based guidance law. In scenario 3, the MD of our method is 12.27 times less than the MD of FBL [1], 1.20 times less than the MD of CMAC-based guidance law, and 1.18 times less than the MD of FBELC-based guidance law. This indicates that our method is superior to recent methods.

In addition, the t-Test statistical analysis is used in this test to propose differences between the methods in Table 4,

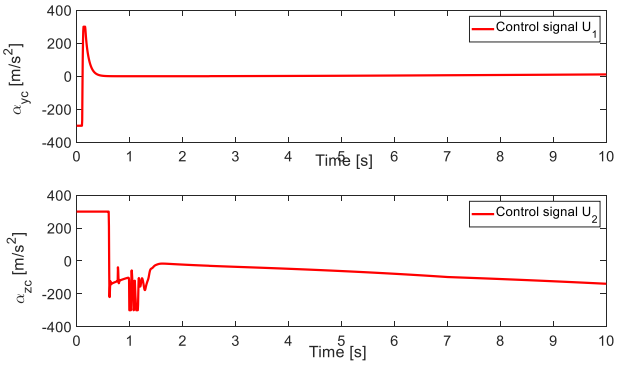

FIGURE 15. Control signal using the proposed method.

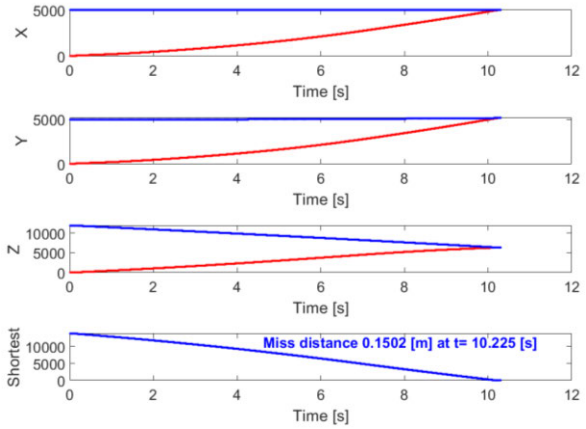

FIGURE 16. Miss distance of missile guidance system with the proposed method.

TABLE 6. Miss-distance comparison for guidance laws.

	Scenario 1	Scenario 2	Scenario 3
Feedback linerizarion Guidance Law (FBL) [1]	4.4539 (m)	3.3578 (m)	1.8434 (m)
Adaptive CMAC based Guidance Law [1]	0.3745 (m)	1.3440 (m)	0.1802 (m)
Adaptive FBELC based Guidance Law	0.3264 (m)	1.26844 (m)	0.1774 (m)
Proposed method	0.2169 (m)	1.1540 (m)	0.1502 (m)

which contains 10,000 continuous samples of our method and Feedback Linearization Guidance Law (FBL), CMAC based guidance law, and FBELC based guidance law.

Remark 4: In Table 7, a comparison of two groups of continuous data, the difference in Means and *P*-values is less than *0.05*. The *t*-Test results between our method and the other controllers show that the Means and *P*-values are acceptable. As a result, the proposed controller differs statistically significantly from the other controllers. *P*-value stands for probability value, *t*_Stat stands for standard-error unit difference, and *df* stands for degrees of freedom.

TABLE 7. The statistical test results for the difference of controllers.

	FBL	Our method	CMAC	Our method	FBLEC	Our method
Mean	0.748	1.24	0.665	1.24	0.615	1.24
Variance	0.005	0.0065	0.0045	0.0065	0.0035	0.0065
df	10		10		10	
t_Stat	5038.1		5038.1		5038.1	
P_value	2.2809×10^{-36}		1.9×10^{-30}		3.45×10^{-20}	
CI	[0.5038 1.1140]		[0.9060 1.1140]		[0.9060 1.1140]	

VI. CONCLUSION

In this study, we have presented the TSKET2FBINN structure for nonlinear systems based on a combination of a type-2 elliptic membership function, a BINN, and a TSK fuzzy inference system. Thus, the TSKET2FBINN structure combines the advantages of the type-2 elliptic membership function, the BINN, and the TSK fuzzy system. The TSKET2FBINN is capable of fast convergence and favorable performance. The TSKET2FBINN parameters are trained using an SMC-based gradient descent algorithm. The stability of the TSKET2FBINN-based control system is demonstrated using a Lyapunov function. Three different scenarios are demonstrated to illustrate the effectiveness of the proposed guidance control system. Under the same conditions, the comparison results show that the proposed method has impressive generalization capability and outperforms other methods in missile guidance control. Future research could include (1) using the optimization algorithm such as modified grey wolf optimizer to determine the optimal learning rates to further improve the learning performance, (2) the development of a self-organization algorithm for the automatically adjusting the structure of TSKET2FBINN for generating the more efficient network structure, and (3) using the proposed TSKET2FBINN for other practical models.

REFERENCES

[1] C.-M. Lin and Y.-F. Peng, "Missile guidance law design using adaptive cerebellar model articulation controller," *IEEE Trans. Neural Netw.*, vol. 16, no. 3, pp. 636–644, May 2005.

[2] C.-L. Lin and T.-L. Wang, "Fuzzy side force control for missile against hypersonic target," *IET Control Theory Appl.*, vol. 1, no. 1, pp. 33–43, Jan. 2007.

[3] C.-H. Wang and K.-N. Hung, "Intelligent adaptive law for missile guidance using fuzzy neural networks," *Int. J. Fuzzy Syst.*, vol. 15, no. 2, pp. 182–191, 2013.

[4] C.-H. Wang, C.-Y. Chen, and K.-N. Hung, "Toward a new task assignment and path evolution (TAPE) for missile defense system (MDS) using intelligent adaptive SOM with recurrent neural networks (RNNs)," *IEEE Trans. Cybern.*, vol. 45, no. 6, pp. 1134–1145, Jun. 2015.

[5] Z. Li, Y. Xia, C.-Y. Su, J. Deng, J. Fu, and W. He, "Missile guidance law based on robust model predictive control using neural-network optimization," *IEEE Trans. Neural Netw. Learn. Syst.*, vol. 26, no. 8, pp. 1803–1809, Aug. 2015.

[6] X. Zhang, H. Xu, Z. Li, F. Shu, and X. Chen, "Adaptive neural piecewise implicit inverse controller design for a class of nonlinear systems considering butterfly hysteresis," *IEEE Trans. Syst., Man, Cybern., Syst.*, vol. 53, no. 6, pp. 3695–3706, Jun. 2023, doi: 10.1109/TSMC.2022.3231261.

[7] R. de Celis and L. Cadarso, "Neural network-based controller for terminal guidance applied in short-range rockets," *IEEE Aerosp. Electron. Syst. Mag.*, vol. 38, no. 4, pp. 28–42, Apr. 2023, doi: 10.1109/MAES.2023.3239342.

[8] R. Su, J. Wang, and S. Zhang, "Design of three-dimensional intelligent guidance law for intercepting highly maneuvering target," *IEEE Access*, vol. 11, pp. 14274–14281, 2023, doi: 10.1109/ACCESS.2023.3241484.

[9] X. Liang, B. Xu, K. Jia, and X. Liu, "Adaptive NN control of integrated guidance and control systems based on disturbance observer," *J. Franklin Inst.*, vol. 360, no. 1, pp. 65–86, Jan. 2023.

[10] X. Bu, B. Jiang, and H. Lei, "Nonfragile quantitative prescribed performance control of waverider vehicles with actuator saturation," *IEEE Trans. Aerosp. Electron. Syst.*, vol. 58, no. 4, pp. 3538–3548, Aug. 2022.

[11] X. Bu, M. Lv, H. Lei, and J. Cao, "Fuzzy neural pseudo control with prescribed performance for waverider vehicles: A fragility-avoidance approach," *IEEE Trans. Cybern.*, early access, Mar. 22, 2023, doi: 10.1109/TCYB.2023.3255925.

[12] C.-F. Juang, R.-B. Huang, and Y.-Y. Lin, "A recurrent self-evolving interval type-2 fuzzy neural network for dynamic system processing," *IEEE Trans. Fuzzy Syst.*, vol. 17, no. 5, pp. 1092–1105, Oct. 2009.

[13] D. Pham, C. Lin, V. N. Giap, T. Huynh, and H. Cho, "Wavelet interval type-2 Takagi-Kang-Sugeno hybrid controller for time-series prediction and chaotic synchronization," *IEEE Access*, vol. 10, pp. 104313–104327, Oct. 2022.

[14] E. Kayacan, A. Sarabakha, S. Coupland, R. John, and M. A. Khanesar, "Type-2 fuzzy elliptic membership functions for modeling uncertainty," *Eng. Appl. Artif. Intell.*, vol. 70, pp. 170–183, Apr. 2018.

[15] J. Mendel, *Uncertain Rule-Based Fuzzy Logic Systems: Introduction and New Directions*. Upper Saddle River, NJ, USA: Prentice-Hall, 2001, p. 555.

[16] J. M. Garibaldi, M. Jaroszewski, and S. Musikasuwan, "New concepts related to non-stationary fuzzy sets," in *Proc. IEEE Int. Fuzzy Syst. Conf.*, Jun. 2007, pp. 1–6.

[17] M. A. Khanesar, E. Kayacan, M. Reyhanoglu, and O. Kaynak, "Feedback error learning control of magnetic satellites using type-2 fuzzy neural networks with elliptic membership functions," *IEEE Trans. Cybern.*, vol. 45, no. 4, pp. 858–868, Apr. 2015.

[18] Z. Deng, Y. Jiang, K.-S. Choi, F.-L. Chung, and S. Wang, "Knowledge-leverage-based TSK fuzzy system modeling," *IEEE Trans. Neural Netw. Learn. Syst.*, vol. 24, no. 8, pp. 1200–1212, Aug. 2013.

[19] J. Zhao and C. Lin, "Wavelet-TSK-type fuzzy cerebellar model neural network for uncertain nonlinear systems," *IEEE Trans. Fuzzy Syst.*, vol. 27, no. 3, pp. 549–558, Mar. 2019.

[20] J. Yoo, J. B. Park, and Y. H. Choi, "Stable predictive control of chaotic systems using self-recurrent wavelet neural network," *Int. J. Control, Autom., Syst.*, vol. 3, no. 1, pp. 43–55, Mar. 2005.

[21] X. Bu and H. Lei, "A fuzzy wavelet neural network-based approach to hypersonic flight vehicle direct nonaffine hybrid control," *Nonlinear Dyn.*, vol. 94, no. 3, pp. 1657–1668, Nov. 2018.

[22] X. Bu, C. Hua, M. Lv, and Z. Wu, "Flight control of waverider vehicles with fragility-avoidance prescribed performance," *IEEE Trans. Aerosp. Electron. Syst.*, early access, Mar. 2, 2023, doi: 10.1109/TAES.2023.3251314.

[23] X. Bu, B. Jiang, and H. Lei, "Low-complexity fuzzy neural control of constrained waverider vehicles via fragility-free prescribed performance approach," *IEEE Trans. Fuzzy Syst.*, early access, Oct. 26, 2022, doi: 10.1109/TFUZZ.2022.3217378.

[24] C. Lucas, D. Shahmirzadi, and N. Sheikholeslami, "Introducing belbic: Brain emotional learning based intelligent controller," *Intell. Autom. Soft Comput.*, vol. 10, no. 1, pp. 11–21, Jan. 2004.

[25] C. Lin, D. Pham, and T. Huynh, "Synchronization of chaotic system using a brain-imitated neural network controller and its applications for secure communications," *IEEE Access*, vol. 9, pp. 75923–75944, 2021.

[26] T.-T. Huynh, C.-M. Lin, D.-H. Pham, N. P. Nguyen, N.-Q.-K. Le, M. T. Vu, V.-P. Vu, and F. Chao, "4-D memristive chaotic systems-based audio secure communication using dual-function-link fuzzy brain emotional controller," *Int. J. Fuzzy Syst.*, vol. 24, no. 6, pp. 2946–2968, Sep. 2022.

[27] C. Lin, D. Pham, and T. Huynh, "Encryption and decryption of audio signal and image secure communications using chaotic system synchronization control by TSK fuzzy brain emotional learning controllers," *IEEE Trans. Cybern.*, vol. 52, no. 12, pp. 13684–13698, Dec. 2022.

[28] F. Chao, D. Zhou, C. Lin, L. Yang, C. Zhou, and C. Shang, "Type-2 fuzzy hybrid controller network for robotic systems," *IEEE Trans. Cybern.*, vol. 50, no. 8, pp. 3778–3792, Aug. 2020.

[29] A. A. Khater, A. M. El-Nagar, M. El-Bardini, and N. El-Rabaie, "A novel structure of actor-critic learning based on an interval type-2 TSK fuzzy neural network," *IEEE Trans. Fuzzy Syst.*, vol. 28, no. 11, pp. 3047–3061, Nov. 2020.

[30] J. Zhang, F. Chao, H. Zeng, C.-M. Lin, and L. Yang, "A recurrent wavelet-based brain emotional learning network controller for nonlinear systems," *Soft Comput.*, vol. 26, pp. 3013–3028, Mar. 2022.

[31] B.-S. Chen, C.-H. Lee, and Y.-C. Chang, "H^{∞} tracking design of uncertain nonlinear SISO systems: Adaptive fuzzy approach," *IEEE Trans. Fuzzy Syst.*, vol. 4, no. 1, pp. 32–43, Feb. 1996.

[32] C.-M. Lin, T.-T. Huynh, and T.-L. Le, "Adaptive TOPSIS fuzzy CMAC back-stepping control system design for nonlinear systems," *Soft Comput.*, vol. 23, no. 16, pp. 6947–6966, Aug. 2019.

[33] H. Lin, H. Zeng, X. Zhang, and W. Wang, "Stability analysis for delayed neural networks via a generalized reciprocally convex inequality," *IEEE Trans. Neural Netw. Learn. Syst.*, early access, Feb. 2, 2022, doi: 10.1109/TNNLS.2022.3144032.

DUC-HUNG PHAM was born in Hung Yen, Vietnam, in 1983. He received the B.S. degree in automatic control and the M.S. degree in automation from the Hanoi University of Science and Technology, Vietnam, in 2006 and 2011, respectively, and the Ph.D. degree from the Department of Electrical Engineering, Yuan Ze University, Chung-Li, Taiwan, in 2022. He is currently a Research Fellow with the Department of Electrical Engineering, Yuan Ze University. He is also a Lecturer with the Faculty of Electrical and Electronic Engineering, Hung Yen University of Technical and Education, Vietnam. His research interests include fuzzy logic control, neural networks, cerebellar model articulation controller, brain emotional learning-based intelligent controller, fault tolerant control, secure communication, and missile guidance control.

CHIH-MIN LIN was born in Changhua, Taiwan, in 1959. He received the B.S. and M.S. degrees from the Department of Control Engineering, National Chiao Tung University, Hsinchu, Taiwan, in 1981 and 1983, respectively, and the Ph.D. degree from the Institute of Electronics Engineering, National Chiao Tung University, in 1986. He is currently a Chair Professor with Yuan Ze University, Taoyuan, Taiwan. From 1997 to 1998, he was an Honorary Research Fellow with the University of Auckland, New Zealand. His research interests include fuzzy neural networks, cerebellar model articulation controller, intelligent control systems, adaptive signal processing, and classification problems. He serves as an Associate Editor for IEEE TRANSACTIONS ON CYBERNETICS and IEEE TRANSACTIONS ON FUZZY SYSTEMS.

VAN NAM GIAP received the B.S. degree in control engineering and automation from the Ha Noi University of Science and Technology, Ha Noi, Vietnam, in 2015, the master's degree in electronic engineering from the National Kaohsiung University of Applied and Sciences, Kaohsiung, Taiwan, in 2017, and the Ph.D. degree in mechanical engineering from the National Kaohsiung University of Science and Technology, Taiwan, in June 2021. He is currently with the Hanoi University of Science and Technology, Vietnam. His research interests include sliding mode control, disturbance and uncertainty estimation, fuzzy logic control, secure communication, magnetic bearing systems and its applications, and self-bearing motors.

VAN-PHONG VU received the B.S. degree from the Department of Automatic Control, Hanoi University of Sciences and Technology, Hanoi, Vietnam, in 2007, the M.S. degree from the Department of Electrical Engineering, Southern Taiwan University of Sciences and Technology, Tainan, Taiwan, in 2010, and the Ph.D. degree from the Department of Electrical Engineering, National Central University, Zhongli, Taiwan, in 2017. He is currently a Lecturer with the Ho Chi Minh City University of Education and Technology, Ho Chi Minh City. His research interests include fuzzy systems, intelligent control, observer and controller design for the uncertain systems, polynomial systems, fault estimation, and large-scale systems.

HSING-YUEH CHO was born in Taiwan, in 1989. He received the master's degree in electrical engineering from the Chien Hsin University of Science and Technology, Zhongli, Taiwan, in 2013. He is currently pursuing the Ph.D. degree in electrical engineering with Yuan Ze University, Taoyuan. His research interests include fuzzy logic control, adaptive control, cerebellar model articulation controllers, and intelligent control systems.